Physics Letters B 716 (2012) 30–61

Contents lists available at SciVerse ScienceDirect

Physics Letters B

www.elsevier.com/locate/physletb

Observation of a new boson at a mass of 125 GeV with the CMS experiment at the LHC ☆

CMS Collaboration *

CERN, Switzerland

This paper is dedicated to the memory of our colleagues who worked on CMS but have since passed away. In recognition of their many contributions to the achievement of this observation.

ARTICLE INFO

Article history:
Received 31 July 2012
Received in revised form 9 August 2012
Accepted 11 August 2012
Available online 18 August 2012
Editor: W.-D. Schlatter

Keywords:
CMS
Physics
Higgs

ABSTRACT

Results are presented from searches for the standard model Higgs boson in proton–proton collisions at $\sqrt{s} = 7$ and 8 TeV in the Compact Muon Solenoid experiment at the LHC, using data samples corresponding to integrated luminosities of up to 5.1 fb^{-1} at 7 TeV and 5.3 fb^{-1} at 8 TeV. The search is performed in five decay modes: $\gamma\gamma$, ZZ, W^+W^-, $\tau^+\tau^-$, and $b\bar{b}$. An excess of events is observed above the expected background, with a local significance of 5.0 standard deviations, at a mass near 125 GeV, signalling the production of a new particle. The expected significance for a standard model Higgs boson of that mass is 5.8 standard deviations. The excess is most significant in the two decay modes with the best mass resolution, $\gamma\gamma$ and ZZ; a fit to these signals gives a mass of $125.3 \pm 0.4(\text{stat.}) \pm 0.5(\text{syst.})$ GeV. The decay to two photons indicates that the new particle is a boson with spin different from one.

1. Introduction

The standard model (SM) of elementary particles provides a remarkably accurate description of results from many accelerator and non-accelerator based experiments. The SM comprises quarks and leptons as the building blocks of matter, and describes their interactions through the exchange of force carriers: the photon for electromagnetic interactions, the W and Z bosons for weak interactions, and the gluons for strong interactions. The electromagnetic and weak interactions are unified in the electroweak theory. Although the predictions of the SM have been extensively confirmed, the question of how the W and Z gauge bosons acquire mass whilst the photon remains massless is still open.

Nearly fifty years ago it was proposed [1–6] that spontaneous symmetry breaking in gauge theories could be achieved through the introduction of a scalar field. Applying this mechanism to the electroweak theory [7–9] through a complex scalar doublet field leads to the generation of the W and Z masses, and to the prediction of the existence of the SM Higgs boson (H). The scalar field also gives mass to the fundamental fermions through the Yukawa interaction. The mass m_H of the SM Higgs boson is not predicted by theory. However, general considerations [10–13] suggest that m_H should be smaller than ∼1 TeV, while precision electroweak measurements imply that $m_H < 152$ GeV at 95% confidence level (CL) [14]. Over the past twenty years, direct searches for the Higgs boson have been carried out at the LEP collider, leading to a lower bound of $m_H > 114.4$ GeV at 95% CL [15], and at the Tevatron proton–antiproton collider, excluding the mass range 162–166 GeV at 95% CL [16] and detecting an excess of events, recently reported in [17–19], in the range 120–135 GeV.

The discovery or exclusion of the SM Higgs boson is one of the primary scientific goals of the Large Hadron Collider (LHC) [20]. Previous direct searches at the LHC were based on data from proton–proton collisions corresponding to an integrated luminosity of 5 fb^{-1} collected at a centre-of-mass energy $\sqrt{s} = 7$ TeV. The CMS experiment excluded at 95% CL a range of masses from 127 to 600 GeV [21]. The ATLAS experiment excluded at 95% CL the ranges 111.4–116.6, 119.4–122.1 and 129.2–541 GeV [22]. Within the remaining allowed mass region, an excess of events near 125 GeV was reported by both experiments. In 2012 the proton–proton centre-of-mass energy was increased to 8 TeV and by the end of June an additional integrated luminosity of more than 5 fb^{-1} had been recorded by each of these experiments, thereby enhancing significantly the sensitivity of the search for the Higgs boson.

This Letter reports the results of a search for the SM Higgs boson using samples collected by the CMS experiment, comprising data recorded at $\sqrt{s} = 7$ and 8 TeV. The search is performed in

☆ © CERN for the benefit of the CMS Collaboration.

* *E-mail address:* cms-publication-committee-chair@cern.ch.

0370-2693/
http://dx.doi.org/10.1016/j.physletb.2012.08.021

five decay modes, $H \to \gamma\gamma$, ZZ, W^+W^-, $\tau^+\tau^-$, and $b\bar{b}$, in the low-mass range from 110 up to 160 GeV. In this mass range the Higgs boson production cross section is predicted to have values between 23 (29) and 10 (14) pb at $\sqrt{s} = 7$ (8) TeV [23]. The natural width of the SM Higgs boson over the same range is less than 100 MeV and the width of any observed peak would be entirely dominated by instrumental mass resolution. In what follows, ℓ stands for electrons or muons, $H \to W^+W^-$ is denoted as $H \to WW$, $H \to \tau^+\tau^-$ as $H \to \tau\tau$, and $H \to b\bar{b}$ as $H \to bb$. For the final states ZZ and WW in the low-mass region, one or more of the Z or W bosons is off mass shell.

With respect to the published analyses [24–28], most analyses have been re-optimized, incorporating improvements in reconstruction performance and event selection, and mitigating the more challenging conditions due to the higher LHC intensities in 2012. The new analyses presented herein, of 8 TeV samples, and of 7 TeV samples featuring modified event selection criteria, were performed in a "blind" way: the algorithms and selection procedures were formally approved and fixed before the results from data in the signal region were examined. In the previously published analyses similar but less formal procedures were followed.

Within the context of this search for the SM Higgs boson, we report the observation of an excess of events above the expected background, consistent with the production of a new particle with mass near 125 GeV. The observed local significance is 5.0 standard deviations (σ), compared with an expected significance of 5.8σ. The evidence is strongest in the two final states with the best mass resolution, namely $H \to \gamma\gamma$ with a significance of 4.1σ and $H \to ZZ$ (with the Z bosons decaying to electrons or muons) with a significance of 3.2σ. The decay to two photons indicates that the new particle is a boson with spin different from one.

2. The CMS experiment

The possibility of detection of the SM Higgs boson played a crucial role in the conceptual design of the CMS experiment as a benchmark to test the performance of the detector [29–31]. Since the SM Higgs boson mass is not predicted by theory and its production cross section and natural width vary widely over the allowed mass range, a search was envisaged over a large range of masses and in diverse decay modes: pairs of photons, Z bosons, W bosons, τ leptons, and b quarks. Planning in view of the analysis of all these channels ensured a detector capable of observing a Higgs boson over a broad mass range and able to detect most potential signals of new physics.

The central feature of the CMS apparatus [32] is a superconducting solenoid of 6 m internal diameter, which provides a magnetic field of 3.8 T. Within the field volume are a silicon pixel and strip tracker, a lead tungstate crystal electromagnetic calorimeter (ECAL), and a brass/scintillator hadron calorimeter (HCAL). Muons are measured in gas-ionization detectors embedded in the steel flux-return yoke. Extensive forward calorimeters complement the coverage provided by the barrel and endcap detectors.

Charged particles are tracked within the pseudorapidity range $|\eta| < 2.5$, where $\eta = -\ln[\tan(\theta/2)]$, and θ is the polar angle measured from the positive z axis (along the anticlockwise beam direction). The silicon pixel tracker comprises 66 million 100×150 μm^2 pixels, arranged in three barrel layers and two disks at each end. The silicon strip tracker, organized in ten barrel layers and twelve disks at each end, comprises 9.3 million strips with pitch between 80 and 180 μm, with a total silicon surface area of 198 m^2. The tracker has a track-finding efficiency larger than 99% for muons with transverse momentum p_T greater than 1 GeV and a transverse momentum resolution between 1.5 and 2.5% for charged tracks of $p_T \sim 100$ GeV in the central region ($|\eta| < 1.5$). Measurements of the impact parameters of charged tracks and secondary vertices are used to identify jets that are likely to contain the hadronisation and decay products of b quarks ("b jets"). A b-jet tagging efficiency of more than 50% is achieved with a rejection factor for light-quark jets of ∼200, as measured in $t\bar{t}$ events in data [33]. The dimuon mass resolution at the Υ mass, dominated by instrumental effects, is measured to be 0.6% in the barrel region [34], consistent with the design goal.

The ECAL is a fine-grained hermetic calorimeter consisting of 75 848 lead tungstate crystals, arranged in a quasi-projective geometry and distributed in a barrel region ($|\eta| < 1.48$) and two endcaps that extend up to $|\eta| = 3.0$. The front-face cross section of the crystals is 22×22 mm^2 in the barrel region and 28.6×28.6 mm^2 in the endcaps. Preshower detectors consisting of two planes of silicon sensors interleaved with a total of three radiation lengths of lead absorber are located in front of the endcaps. Electromagnetic showers are very narrow in lead tungstate (Molière radius of 21 mm), helping in particle identification and in the implementation of isolation criteria. In the central barrel region the energy resolution of electrons that do not radiate substantially in the tracker material indicates that the resolution of unconverted photons is consistent with design goals. For such photons the diphoton mass resolution is 1.1 GeV at a mass of 125 GeV.

The HCAL barrel and endcaps are sampling calorimeters consisting of brass and scintillator plates, covering $|\eta| < 3.0$. Their thickness varies from 7 to 11 interaction lengths, depending on η; a scintillator "tail catcher" placed outside the coil of the solenoid, just in front of the innermost muon detector, extends the instrumented thickness to more than 10 interaction lengths everywhere. Iron forward calorimeters with quartz fibers, read out by photomultipliers, extend the calorimeter coverage up to $|\eta| = 5.0$.

Muons are measured in the range $|\eta| < 2.4$, with detection planes based on three technologies: drift tubes ($|\eta| < 1.2$), cathode strip chambers ($0.9 < |\eta| < 2.4$), and resistive plate chambers ($|\eta| < 1.6$). The first two technologies provide a precise position measurement and trigger whilst the third provides precise timing information as well as a second and independent trigger. The muon system consists of four stations in the barrel and endcaps, designed to ensure robust triggering and detection of muons over a large angular range. In the barrel region each muon station consists of twelve drift-tube layers, except for the outermost station, which has eight layers. In the endcaps, each muon station consists of six detection planes. The precision of the r–ϕ measurement is 100 μm in the drift tubes and varies from 60 to 140 μm in the cathode strip chambers.

The CMS trigger and data acquisition systems ensure that potentially interesting events are recorded with high efficiency. The first level (L1) trigger, comprising the calorimeter, muon, and global trigger processors, uses coarse-granularity information to select the most interesting events in less than 4 μs. The detector data are pipelined to ensure negligible deadtime up to a L1 rate of 100 kHz. After L1 triggering, data are transferred from the readout electronics of all subdetectors, through the readout network, to the high-level-trigger processor farm, which operates offline-quality reconstruction algorithms to decrease the event rate to around 0.5 kHz, before data storage.

The CMS experiment employs a highly distributed computing infrastructure, with a primary Tier-0 centre at CERN, supplemented by seven Tier-1, more than 50 Tier-2, and many Tier-3 centres at national laboratories and universities throughout the world. The CMS software running on this high-performance computing system executes numerous tasks, including the reconstruction and analysis of the collected data, as well as the generation and detailed detector simulation of Monte Carlo (MC) event samples.

3. Event reconstruction

The CMS "particle-flow" event description algorithm [35,36] is used to reconstruct and identify each single particle with an optimized combination of all subdetector information. In this process, the identification of the particle (photon, electron, muon, charged hadron, neutral hadron) plays an important role in the determination of the particle momentum. The reconstructed particles are henceforth referred to as objects.

Jets are reconstructed by clustering the particle-flow objects with the anti-k_T algorithm [37] using a distance parameter of 0.5. Additional selection criteria are applied to each event to remove spurious features originating from isolated noise patterns in certain HCAL regions, and from anomalous signals caused by particles depositing energy in the silicon avalanche photodiodes used in the ECAL barrel region. The average number of pp interactions per LHC bunch crossing is estimated to be about 9 and 19 in the 7 TeV (2011) and 8 TeV (2012) data sets, respectively. Energy from overlapping pp interactions ("pileup"), and from the underlying event, is subtracted using the FastJet technique [38–40], which is based on the calculation of the η-dependent transverse momentum density, evaluated on an event-by-event basis.

The jet momentum is determined as the vector sum of all particle momenta in the jet. Jet energy corrections are derived from simulation studies and from in situ measurements using the energy balance of dijet and Z/γ + jet events [41]. These corrections are between 5% and 10% of the true momentum over the entire p_T spectrum and detector acceptance. The jet momentum resolution achieved is $\sigma(p_T)/p_T = 85\%/\sqrt{p_T/\text{GeV}} \oplus 4\%$ for central jets. A selection is applied to separate jets originating in the primary interaction from those due to energy deposits associated with pileup. The discrimination is based on the differences in the jet shapes, in the relative multiplicity of charged and neutral components, and in the fraction of transverse momentum carried by the hardest components. Within the tracker acceptance the jet tracks are also required to be consistent with originating at the primary vertex.

The missing transverse energy vector is taken as the negative vector sum of all particle transverse momenta, and its magnitude is referred to as E_T^{miss}. The typical missing transverse energy resolution is around $0.5\sqrt{\sum E_T}$ GeV [42], where $\sum E_T$ is the scalar sum of all particle transverse momenta in GeV.

The energy deposited in the ECAL is clustered both with general clustering algorithms [43] and with algorithms that constrain the clusters in η and ϕ to the shapes expected from electrons and photons with high p_T [44]. These specialised algorithms are used to cluster electromagnetic showers without any hypothesis regarding whether the particle originating from the interaction point was a photon or an electron; doing this for electrons from $Z \to ee$ events provides a measurement of the photon trigger, reconstruction, and identification efficiencies, as well as of the photon energy scale and resolution. The width of the reconstructed Z resonance is used to quantify the performance of the ECAL, using decays to two electrons whose energies are measured using the ECAL alone, with only their directions being determined from the tracks. In the 7 TeV data set, the dielectron mass resolution at the Z boson mass is 1.56 GeV in the barrel and 2.57 GeV in the endcaps, while in the 8 TeV sample, reconstructed with preliminary calibration constants, the corresponding values are 1.61 and 3.75 GeV. For electrons, the reconstruction combines the clusters in the ECAL and the trajectory in the silicon tracker [45]. Trajectories in the tracker volume are reconstructed using a model of electron energy loss and fitted with a Gaussian sum filter [46]. The electron momentum is determined from the combination of ECAL and tracker measurements.

Table 1
Summary of the subchannels, or categories, used in the analysis of each decay mode.

Decay mode	Production tagging	No. of subchannels	m_H range (GeV)	Int. Lum. (fb^{-1})	
				7 TeV	8 TeV
$\gamma\gamma$	untagged	4	110–150	5.1	5.3
	dijet (VBF)	1 or 2			
ZZ	untagged	3	110–160	5.1	5.3
WW	untagged	4	110–160	4.9	5.1
	dijet (VBF)	1 or 2			
$\tau\tau$	untagged	16	110–145	4.9	5.1
	dijet (VBF)	4			
bb	lepton, E_T^{miss} (VH)	10	110–135	5.0	5.1

Muon candidates are reconstructed with two algorithms, one in which the tracks in the silicon detector are matched to segments in the muon chambers, and another in which a combined fit is performed to the signals found in both the silicon tracker and muon systems [43]. The efficiency to reconstruct a muon of $p_T > 5$ GeV is larger than 95%, while the probability to misidentify a hadron as a muon is below 0.1%. For $p_T > 200$ GeV the precision of the momentum measurement improves when the silicon tracker signals are complemented with the information from the muon chambers.

Selection based on isolation of lepton and photon objects is used extensively. A requirement is placed on the scalar sum of the transverse momenta of the particles reconstructed within a distance ΔR_{max} of the object, sometimes normalised to the p_T of the object. The distance ΔR is defined as $\Delta R = \sqrt{(\Delta\eta)^2 + (\Delta\phi)^2}$, where $\Delta\eta$ and $\Delta\phi$ are the pseudorapidity and azimuthal angle differences between the particle direction and the object direction. Typically ΔR_{max} is chosen to be 0.3 or 0.4.

The measurement of the integrated luminosity in CMS is based on a pixel cluster counting method, which exploits the large number of silicon pixels, and hence their low occupancy in a pp collision [47]. The cross section normalisation is derived from van der Meer scans [48]. The uncertainties in the luminosity measurements are 2.2% and 4.4% for the 7 TeV and 8 TeV data sets, respectively.

4. Searches for the standard model Higgs boson

Initial phenomenological discussions of Higgs boson production and decay can be found in Refs. [49–56]. Four main mechanisms are predicted for Higgs boson production in pp collisions: the gluon–gluon fusion mechanism, which has the largest cross section, followed in turn by vector-boson fusion (VBF), associated WH and ZH production (VH), and production in association with top quarks ($t\bar{t}H$). The cross sections for the individual production mechanisms and the decay branching fractions, together with their uncertainties, have been computed following Refs. [57–101] and are compiled in Refs. [23,102].

The particular set of sensitive decay modes of the SM Higgs boson depends strongly on m_H. The results presented in this Letter are based on the five most sensitive decay modes in the low-mass region: $H \to \gamma\gamma$; $H \to ZZ$ followed by ZZ decays to 4ℓ; $H \to WW$ followed by decays to $2\ell 2\nu$; $H \to \tau\tau$ followed by at least one leptonic τ decay; and $H \to bb$ followed by b-quark fragmentation into jets. This list is presented in Table 1 and comprises the full set of decay modes and subchannels, or categories, for which both the 7 and 8 TeV data sets have been analysed. Other lower sensitivity subchannels ($t\bar{t}H$, $H \to bb$; W/ZH, $H \to \tau\tau$; W/ZH, $H \to WW \to 2\ell 2\nu$; $H \to ZZ \to 2\ell 2q$) have also been studied, so far only in the 7 TeV data, and are not included here. Adding these analyses in the combination results in an improvement of 0.1σ in the overall expected local significance at $m_H = 125$ GeV.

For a given value of m_H, the search sensitivity depends on the production cross section, the decay branching fraction into the chosen final state, the signal selection efficiency, the mass resolution, and the level of background from identical or similar final-state topologies.

Samples of MC events used to represent signal and background are fully simulated using GEANT4 [103]. The simulations include pileup interactions matching the distribution of the number of such interactions observed in data. The description of the Higgs boson signal is obtained from MC simulation using, for most of the decay modes and production processes, the next-to-leading-order (NLO) matrix-element generator POWHEG [104,105], interfaced with PYTHIA 6.4 [106]. For the dominant gluon–gluon fusion process, the transverse momentum spectrum of the Higgs boson in the 7 TeV MC samples is reweighted to the next-to-next-to-leading-logarithmic (NNLL) + NLO distribution computed with HQT [71,72,107] and FEHIPRO [108,109], except in the $H \to ZZ$ analysis, where the effect is marginal. The agreement of the p_T spectrum in the simulation at 8 TeV with the NNLL + NLO distribution makes reweighting unnecessary. The improved agreement is due to a modification in the POWHEG setup recommended in Ref. [102]. The simulation of associated-production signal samples uses PYTHIA and all signal samples for $H \to bb$ are made using POWHEG interfaced to HERWIG++ [110]. Samples used for background studies are generated with PYTHIA, POWHEG, and MADGRAPH [111], and the normalisations are obtained from the best available NNLO or NLO calculations. The uncertainty in the signal cross section related to the choice of parton distribution functions is determined with the PDF4LHC prescription [96–100].

The overall statistical methodology [112] used in this Letter was developed by the CMS and ATLAS Collaborations in the context of the LHC Higgs Combination Group. A more concise summary of CMS usage in the search for a Higgs boson is given in Ref. [21]. The modified frequentist criterion CL_s [113,114] is used for the calculation of exclusion limits. Systematic uncertainties are incorporated as nuisance parameters and are treated according to the frequentist paradigm. The combination of searches requires simultaneous analysis of the data selected by all individual analyses, accounting for all statistical and systematic uncertainties and their correlations. The probability for a background fluctuation to be at least as large as the observed maximum excess is termed the local p-value, and that for an excess *anywhere* in a specified mass range the global p-value. This probability can be evaluated by generating sets of simulated data incorporating all correlations between analyses optimized for different Higgs boson masses. The global p-value (for the specified region) is greater than the local p-value, and this fact is often referred to as the look-elsewhere effect (LEE) [115]. Both the local and global p-values can be expressed as a corresponding number of standard deviations using the one-sided Gaussian tail convention. The magnitude of a possible Higgs boson signal is characterised by the production cross section times the relevant branching fractions, relative to the SM expectation, denoted σ/σ_{SM} and referred to as the signal strength. The results presented in this Letter are obtained using asymptotic formulae [116], including updates recently introduced in the ROOSTATS package [117].

Fig. 1 shows the expected local p-values in the mass range 110–145 GeV for the five decay modes reported here. The expected significance of a SM Higgs boson signal at $m_H = 125$ GeV when the five decay modes are combined is 5.6σ. The highest sensitivity in this mass range is achieved in the ZZ, $\gamma\gamma$, and WW channels. Because of the excellent mass resolution (1–2 GeV) achieved in the $\gamma\gamma$ and ZZ channels, they play a special role in the low-mass region, where the natural width of the SM Higgs boson is predicted to be less than 100 MeV. The expected signature in these channels is therefore a narrow resonance above background, with a width consistent with the detector resolution.

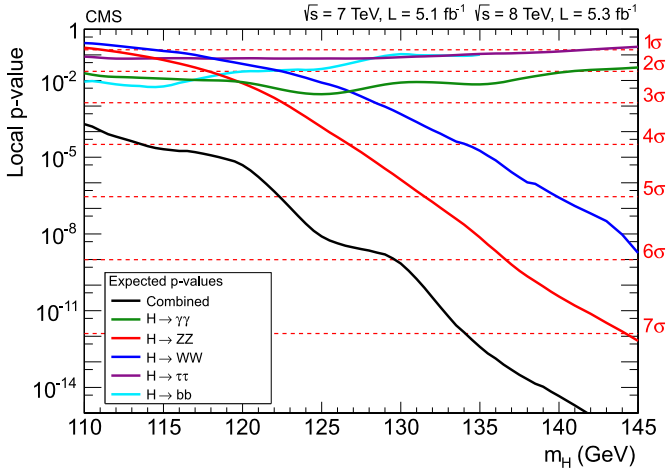

Fig. 1. Expected local p-values for a SM Higgs boson as a function of m_H, for the decay modes $\gamma\gamma$, ZZ, WW, $\tau\tau$, and bb and their combination.

5. Decay modes with high mass resolution

5.1. $H \to \gamma\gamma$

In the $H \to \gamma\gamma$ analysis a search is made for a narrow peak in the diphoton invariant mass distribution in the range 110–150 GeV, on a large irreducible background from QCD production of two photons. There is also a reducible background where one or more of the reconstructed photon candidates originate from misidentification of jet fragments. Early detailed studies indicated this to be one of the most promising channels in the search for a SM Higgs boson in the low-mass range [118].

To enhance the sensitivity of the analysis, candidate diphoton events are separated into mutually exclusive categories of different expected signal-to-background ratios, based on the properties of the reconstructed photons and on the presence of two jets satisfying criteria aimed at selecting events in which a Higgs boson is produced through the VBF process. The analysis uses multivariate techniques for the selection and classification of the events. As an independent cross-check, an analysis is also performed that is almost identical to the one described in Ref. [24], using simpler criteria based on the properties of the reconstructed photons to select and classify events. The multivariate analysis achieves 15% higher sensitivity than the cross-check analysis.

The reconstructed primary vertex that most probably corresponds to the interaction vertex of the diphoton candidate is identified using the kinematic properties of the tracks associated with that vertex and their correlation with the diphoton kinematics. In addition, if either of the photons converts and the tracks from the conversion are reconstructed and identified, the direction of the converted photon contributes to the identification of the hard-scattering vertex. More details can be found in Ref. [24].

The event selection requires two photon candidates satisfying p_T requirements and "loose" photon identification criteria. These photons must be reconstructed within the fiducial region, $|\eta| < 2.5$, excluding the barrel–endcap transition region, $1.44 < |\eta| < 1.57$. A p_T threshold of $m_{\gamma\gamma}/3$ ($m_{\gamma\gamma}/4$) is applied to the photon leading (subleading) in p_T, where $m_{\gamma\gamma}$ is the diphoton invariant mass. Scaling the p_T thresholds in this way avoids distortion of the shape of the $m_{\gamma\gamma}$ distribution. In the case of events passing the dijet selection, the requirement on the leading photon

Table 2
Expected numbers of SM Higgs boson events ($m_H = 125$ GeV) and estimated background (at $m_{\gamma\gamma} = 125$ GeV) for all event categories of the 7 and 8 TeV data sets. There are two dijet-tagged categories for the 8 TeV data as described in the text, and for both data sets the remaining untagged events are separated into four categories labelled here BDT 0–3, BDT 0 having the largest expected signal-to-background ratio. The composition of the SM Higgs boson signal in terms of the production processes, and its mass resolution, are also given.

Event categories		SM Higgs boson expected signal ($m_H = 125$ GeV)							Background $m_{\gamma\gamma} = 125$ GeV (events/GeV)
		Events	ggH	VBF	VH	ttH	σ_{eff} (GeV)	FWHM/2.35 (GeV)	
7 TeV, 5.1 fb^{-1}	BDT 0	3.2	61%	17%	19%	3%	1.21	1.14	3.3 ± 0.4
	BDT 1	16.3	88%	6%	6%	–	1.26	1.08	37.5 ± 1.3
	BDT 2	21.5	92%	4%	4%	–	1.59	1.32	74.8 ± 1.9
	BDT 3	32.8	92%	4%	4%	–	2.47	2.07	193.6 ± 3.0
	Dijet tag	2.9	27%	72%	1%	–	1.73	1.37	1.7 ± 0.2
8 TeV, 5.3 fb^{-1}	BDT 0	6.1	68%	12%	16%	4%	1.38	1.23	7.4 ± 0.6
	BDT 1	21.0	87%	6%	6%	1%	1.53	1.31	54.7 ± 1.5
	BDT 2	30.2	92%	4%	4%	–	1.94	1.55	115.2± 2.3
	BDT 3	40.0	92%	4%	4%	–	2.86	2.35	256.5 ± 3.4
	Dijet tight	2.6	23%	77%	–	–	2.06	1.57	1.3 ± 0.2
	Dijet loose	3.0	53%	45%	2%	–	1.95	1.48	3.7 ± 0.4

is increased to $m_{\gamma\gamma}/2$, further reducing background with negligible loss of signal.

Jet selection criteria are applied to the two jets of largest p_T in the event within $|\eta| < 4.7$. The jet selection requirements are optimized using simulated VBF signal and diphoton background events. The p_T thresholds for the two jets are 30 and 20 GeV, and their η separation is required to be greater than 3.5. The dijet invariant mass is required to be greater than 350 and 250 GeV for the 7 and 8 TeV data sets, respectively. The lower dijet invariant mass requirement for the 8 TeV data set reflects the fact that for the analysis of that data set, the dijet event category is divided into two to increase the search sensitivity. This division creates a second "tight" dijet-tagged category in which the dijet invariant mass must be greater than 500 GeV and both jets must have $p_T > 30$ GeV. Two additional selection criteria, relating the dijet to the diphoton system, are applied: the difference between the average pseudorapidity of the two jets and the pseudorapidity of the diphoton system is required to be less than 2.5, and the difference in azimuthal angle between the diphoton system and the dijet system is required to be greater than 2.6 radians.

A multivariate regression is used to extract the photon energy and a photon-by-photon estimate of the uncertainty in that measurement. The calibration of the photon energy scale uses the Z boson mass as a reference; ECAL showers coming from electrons in $Z \to ee$ events are clustered and reconstructed in exactly the same way as photon showers. The photon selection efficiency, energy resolution, and associated systematic uncertainties are estimated from data, using $Z \to ee$ events to derive data/simulation correction factors. The jet reconstruction efficiency, the efficiency to correctly locate the vertex position, and the trigger efficiency, together with the corresponding systematic uncertainties, are also evaluated from data.

For the multivariate analysis, a boosted decision tree (BDT) [119,120] is trained to give a high output value (score) for signal-like events and for events with good diphoton invariant mass resolution, based on the following observables: (i) the photon quality determined from electromagnetic shower shape and isolation variables; (ii) the expected mass resolution; (iii) the per-event estimate of the probability of locating the diphoton vertex within 10 mm of its true location along the beam direction; and (iv) kinematic characteristics of the photons and the diphoton system. The kinematic variables are constructed so as to contain no information about the invariant mass of the diphoton system. The diphoton events not satisfying the dijet selection are classified into five categories based on the output of the BDT, with category boundaries optimized for sensitivity to a SM Higgs boson. Events in the category with smallest expected signal-to-background ratio are rejected, leaving four categories of events. Dijet-tagged events with BDT scores smaller than the threshold for the fourth category are also rejected. Simulation studies indicate that the background in the selected event categories is dominated by the irreducible background from QCD production of two photons and that fewer than 30% of the diphoton events used in the analysis contain one or more misidentified photons (predominantly from γ + jet production).

Table 2 shows the expected number of signal events in each event category for a SM Higgs boson (of $m_H = 125$ GeV), and the background at $m_{\gamma\gamma} = 125$ GeV, estimated from the fit described below. The estimated mass resolution is also shown, measured both by σ_{eff}, half the minimum width containing 68% of the signal events, and by the full width at half maximum (FWHM). A large variation in the expected signal-to-background ratio between the categories can be seen, although as a consequence of the optimization of the category boundaries the expected signal significances in each category are rather similar. The differences in the relative signal-to-background ratio between the categories are almost independent of m_H.

The background is estimated from data, without the use of MC simulation, by fitting the diphoton invariant mass distribution in each of the categories in a range ($100 < m_{\gamma\gamma} < 180$ GeV) extending slightly above and below that in which the search is performed. The choices of the function used to model the background and of the fit range are made based on a study of the possible bias in the measured signal strength. Polynomial functions are used. The degree is chosen by requiring that the potential bias be at least a factor of 5 smaller than the statistical accuracy of the fit prediction. The required polynomial degree ranges from 3 to 5.

A further independent analysis (referred to as the sideband background model) is performed using a different approach to the background modelling. Its sensitivity is very similar to that of the standard analysis. It employs a fit to the output of an additional BDT that takes as input the diphoton invariant mass and the diphoton BDT output, and uses a background model derived from the sidebands of the invariant mass distribution. A fit to the diphoton invariant mass distribution is used to obtain the background normalisation. This fit is of a power law and excludes a window of width $\pm 2\% \times m_H$ around the mass hypothesis. The methodology allows a systematic uncertainty to be assigned to the fit shape.

The expected 95% CL upper limit on the signal strength σ/σ_{SM}, in the background-only hypothesis, for the combined 7 and 8 TeV data, is less than 1.0 in the range $110 < m_H < 140$ GeV, with a value of 0.76 at $m_H = 125$ GeV. The observed limit indicates the

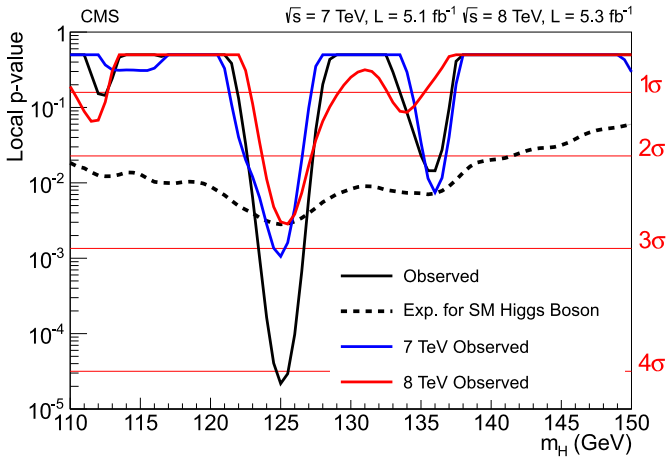

Fig. 2. The local p-value as a function of m_{H} in the $\gamma\gamma$ decay mode for the combined 7 and 8 TeV data sets. The additional lines show the values for the two data sets taken individually. The dashed line shows the expected local p-value for the combined data sets, should a SM Higgs boson exist with mass m_{H}.

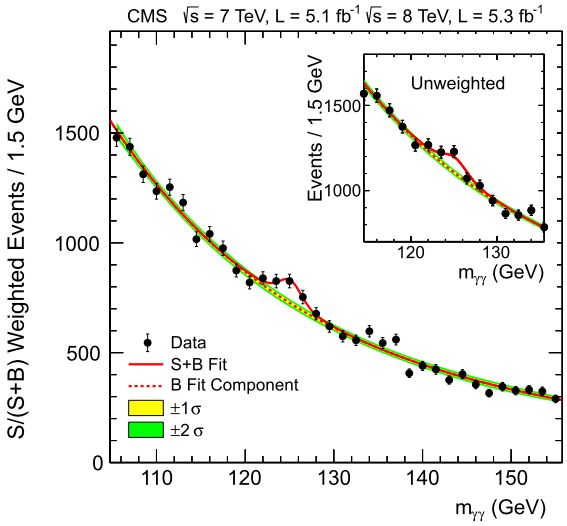

Fig. 3. The diphoton invariant mass distribution with each event weighted by the $S/(S+B)$ value of its category. The lines represent the fitted background and signal, and the coloured bands represent the ±1 and ±2 standard deviation uncertainties in the background estimate. The inset shows the central part of the unweighted invariant mass distribution. (For interpretation of the references to colour in this figure legend, the reader is referred to the web version of this Letter.)

presence of a significant excess at $m_{\mathrm{H}} = 125$ GeV in both the 7 and 8 TeV data. The features of the observed limit are confirmed by the independent sideband-background-model and cross-check analyses. The local p-value is shown as a function of m_{H} in Fig. 2 for the 7 and 8 TeV data, and for their combination. The expected (observed) local p-value for a SM Higgs boson of mass 125 GeV corresponds to $2.8(4.1)\sigma$. In the sideband-background-model and cross-check analyses, the observed local p-values for $m_{\mathrm{H}} = 125$ GeV correspond to 4.6 and 3.7σ, respectively. The best-fit signal strength for a SM Higgs boson mass hypothesis of 125 GeV is $\sigma/\sigma_{\mathrm{SM}} = 1.6 \pm 0.4$.

In order to illustrate, in the $m_{\gamma\gamma}$ distribution, the significance given by the statistical methods, it is necessary to take into account the large differences in the expected signal-to-background ratios of the event categories shown in Table 2. The events are weighted according to the category in which they fall. A weight proportional to $S/(S+B)$ is used, as suggested in Ref. [121], where S and B are the number of signal and background events, respectively, calculated from the simultaneous signal-plus-background fit to all categories (with varying overall signal strength) and integrating over a $2\sigma_{\mathrm{eff}}$ wide window, in each category, centred on 125 GeV. Fig. 3 shows the data, the signal model, and the background model, all weighted. The weights are normalised such that the integral of the weighted signal model matches the number of signal events given by the best fit. The unweighted distribution, using the same binning but in a more restricted mass range, is shown as an inset. The excess at 125 GeV is evident in both the weighted and unweighted distributions.

5.2. $\mathrm{H} \to \mathrm{ZZ}$

In the $\mathrm{H} \to \mathrm{ZZ} \to 4\ell$ decay mode a search is made for a narrow four-lepton mass peak in the presence of a small continuum background. Early detailed studies outlined the promise of this mode over a wide range of Higgs boson masses [122]. Only the search in the range 110–160 GeV is reported here. Since there are differences in the reducible background rates and mass resolutions between the subchannels 4e, 4μ, and $2e2\mu$, they are analysed separately. The background sources include an irreducible four-lepton contribution from direct ZZ production via $\mathrm{q\bar{q}}$ and gluon–gluon processes. Reducible contributions arise from $\mathrm{Z}+\mathrm{b\bar{b}}$ and $\mathrm{t\bar{t}}$ production where the final states contain two isolated leptons and two b-quark jets producing secondary leptons. Additional background arises from Z + jets and WZ + jets events where jets are misidentified as leptons. Compared to the analysis reported in Ref. [25], the present analysis employs improved muon reconstruction, improved lepton identification and isolation, and a kinematic discriminant exploiting the decay kinematics expected for the signal events. An algorithm to recover final-state radiation (FSR) photons has also been deployed.

Electrons are required to have $p_{\mathrm{T}} > 7$ GeV and $|\eta| < 2.5$. The corresponding requirements for muons are $p_{\mathrm{T}} > 5$ GeV and $|\eta| < 2.4$. Electrons are selected using a multivariate identifier trained using a sample of W + jets events, and the working point is optimized using Z + jets events. Both muons and electrons are required to be isolated. The combined reconstruction and selection efficiency is measured using electrons and muons in Z boson decays. Muon reconstruction and identification efficiency for muons with $p_{\mathrm{T}} < 15$ GeV is measured using J/ψ decays.

The electron or muon pairs from Z boson decays are required to originate from the same primary vertex. This is ensured by requiring that the significance of the impact parameter with respect to the event vertex satisfy $|S_{\mathrm{IP}}| < 4$ for each lepton, where $S_{\mathrm{IP}} = I/\sigma_I$, I is the three-dimensional lepton impact parameter at the point of closest approach to the vertex, and σ_I its uncertainty.

Final-state radiation from the leptons is recovered and included in the computation of the lepton-pair invariant mass. The FSR recovery is tuned using simulated samples of $\mathrm{ZZ} \to 4\ell$ and tested on data samples of Z boson decays to electrons and muons. Photons reconstructed within $|\eta| < 2.4$ are considered as possibly due to FSR. The photons must satisfy the following requirements. They must be within $\Delta R < 0.07$ of a muon and have $p_{\mathrm{T}}^{\gamma} > 2$ GeV (most photon showers within this distance of an electron having already been automatically clustered with the electron shower); or if their distance from a lepton is in the range $0.07 < \Delta R < 0.5$, they must satisfy $p_{\mathrm{T}}^{\gamma} > 4$ GeV, and be isolated within $\Delta R = 0.3$. Such photon candidates are combined with the lepton if the resulting three-body invariant mass is less than 100 GeV and closer to the Z boson mass than the mass before the addition of the photon.

The event selection requires two pairs of same-flavour, oppositely charged leptons. The pair with invariant mass closest to the Z boson mass is required to have a mass in the range 40–120 GeV

Table 3
The number of selected events, compared to the expected background yields and expected number of signal events ($m_H = 125$ GeV) for each final state in the $H \to ZZ$ analysis. The estimates of the $Z + X$ background are based on data. These results are given for the mass range from 110 to 160 GeV. The total background and the observed numbers of events are also shown for the three bins ("signal region") of Fig. 4 where an excess is seen ($121.5 < m_{4\ell} < 130.5$ GeV).

Channel	4e	4μ	$2e2\mu$	4ℓ
ZZ background	2.7 ± 0.3	5.7 ± 0.6	7.2 ± 0.8	15.6 ± 1.4
$Z + X$	$1.2^{+1.1}_{-0.8}$	$0.9^{+0.7}_{-0.6}$	$2.3^{+1.8}_{-1.4}$	$4.4^{+2.2}_{-1.7}$
All backgrounds ($110 < m_{4\ell} < 160$ GeV)	4.0 ± 1.0	6.6 ± 0.9	9.7 ± 1.8	20 ± 3
Observed ($110 < m_{4\ell} < 160$ GeV)	6	6	9	21
Signal ($m_H = 125$ GeV)	1.36 ± 0.22	2.74 ± 0.32	3.44 ± 0.44	7.54 ± 0.78
All backgrounds (signal region)	0.7 ± 0.2	1.3 ± 0.1	1.9 ± 0.3	3.8 ± 0.5
Observed (signal region)	1	3	5	9

and the other pair is required to have a mass in the range 12–120 GeV. The ZZ background is evaluated from MC simulation studies. Two different approaches are employed to estimate the reducible and instrumental backgrounds from data. Both start by selecting events in a background control region, well separated from the signal region, by relaxing the isolation and identification criteria for two same-flavour reconstructed leptons. In the first approach, the additional pair of leptons is required to have the same charge (to avoid signal contamination) while in the second, two opposite-charge leptons failing the isolation and identification criteria are required. In addition, a control region with three passing leptons and one failing lepton is used to estimate contributions from backgrounds with three prompt leptons and one misidentified lepton. The event rates measured in the background control region are extrapolated to the signal region using the measured probability for a reconstructed lepton to pass the isolation and identification requirements. This probability is measured in an independent sample. Within uncertainties, comparable background counts in the signal region are estimated by both methods.

The number of selected $ZZ \to 4\ell$ candidate events in the mass range $110 < m_{4\ell} < 160$ GeV, in each of the three final states, is given in Table 3, where $m_{4\ell}$ is the four-lepton invariant mass. The number of predicted background events, in each of the three final states, and their uncertainties are also given, together with the number of signal events expected from a SM Higgs boson of $m_H = 125$ GeV. The $m_{4\ell}$ distribution is shown in Fig. 4. There is a clear peak at the Z boson mass where the decay $Z \to 4\ell$ is reconstructed. This feature of the data is well reproduced by the background estimation. The figure also shows an excess of events above the expected background around 125 GeV. The total background and the numbers of events observed in the three bins where an excess is seen are also shown in Table 3. The combined signal reconstruction and selection efficiency, with respect to the $m_H = 125$ GeV generated signal with $m_{\ell\ell} > 1$ GeV as the only cut, is 18% for the 4e channel, 40% for the 4μ channel, and 27% for the $2e2\mu$ channel.

The kinematics of the $H \to ZZ \to 4\ell$ process in its centre-of-mass frame, for a given invariant mass of the four-lepton system, is fully described by five angles and the invariant masses of the two lepton pairs [123–125]. These seven variables provide significant discriminating power between signal and background. The momentum of the ZZ system may further differentiate signal from background, but would introduce dependence on the production mechanism, and on the modelling of the QCD effects, and is therefore not considered here. A kinematic discriminant is constructed based on the probability ratio of the signal and background hypotheses, $K_D = \mathcal{P}_{sig}/(\mathcal{P}_{sig} + \mathcal{P}_{bkg})$, as described in Ref. [126]. The likelihood ratio is defined for each value of $m_{4\ell}$. For the signal, the phase-space and Z propagator terms [127] are included in a fully analytic parameterization [124], while the background probability

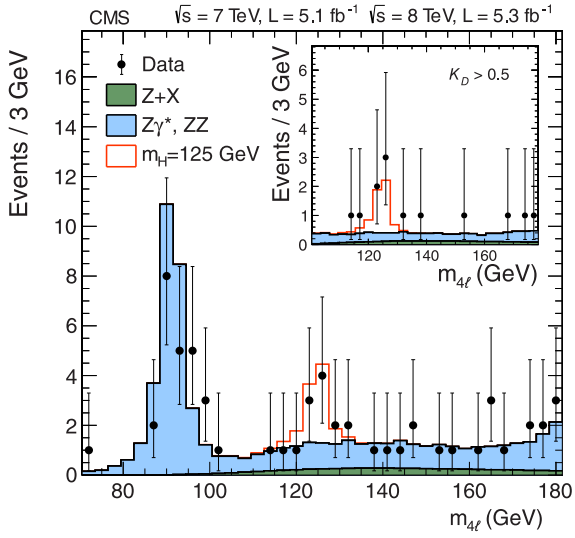

Fig. 4. Distribution of the four-lepton invariant mass for the $ZZ \to 4\ell$ analysis. The points represent the data, the filled histograms represent the background, and the open histogram shows the signal expectation for a Higgs boson of mass $m_H = 125$ GeV, added to the background expectation. The inset shows the $m_{4\ell}$ distribution after selection of events with $K_D > 0.5$, as described in the text.

is tabulated using a simulation of the $q\bar{q} \to ZZ/Z\gamma$ process. The statistical analysis only includes events with $m_{4\ell} > 100$ GeV.

Fig. 5 (upper) shows the distribution of K_D versus $m_{4\ell}$ for events selected in the 4ℓ subchannels. The colour-coded regions show the expected background. Fig. 5 (lower) shows the same two-dimensional distribution of events, but this time superimposed on the expected event density from a SM Higgs boson ($m_H = 125$ GeV). A clustering of events is observed around 125 GeV with a large value of K_D, where the background expectation is low and the signal expectation is high, corresponding to the excess seen in the one-dimensional mass distribution. The $m_{4\ell}$ distribution of events satisfying $K_D > 0.5$ is shown in the inset in Fig. 4.

There are three final states and two data sets (7 and 8 TeV), and thus the statistical treatment requires six simultaneous two-dimensional maximum-likelihood fits for each value of m_H, in the variables $m_{4\ell}$ and K_D. Systematic uncertainties are evaluated from data for the trigger efficiency and for the combined lepton reconstruction, identification, and isolation efficiencies, as described in [128]. Systematic uncertainties in the energy/momentum calibration and in the energy resolution are estimated from data. Additional systematic uncertainties arise from limited statistical precision in the reducible background control regions.

The expected 95% CL upper limit on the signal strength σ/σ_{SM}, in the background-only hypothesis, for the combined 7 and 8 TeV

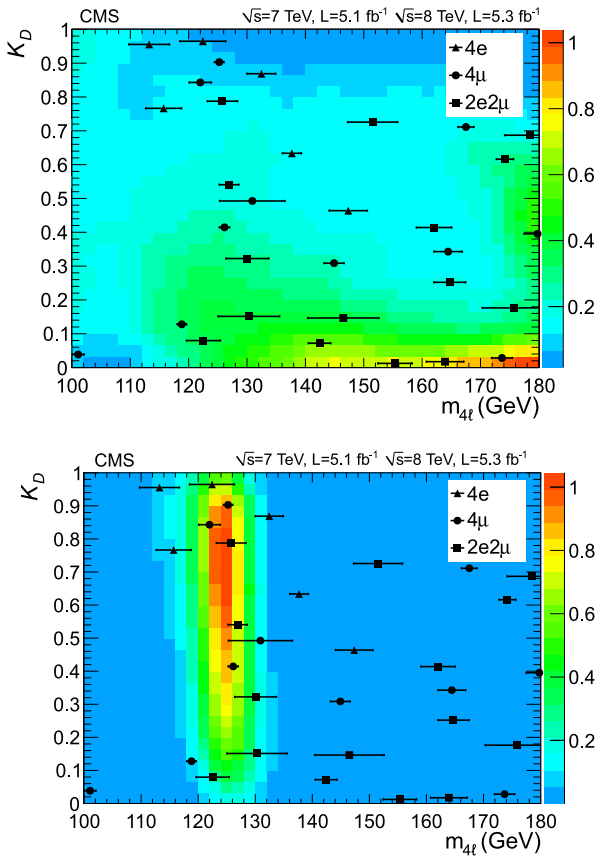

Fig. 5. The distribution of events selected in the 4ℓ subchannels for the kinematic discriminant K_D versus $m_{4\ell}$. Events in the three final states are marked by filled symbols (defined in the legend). The horizontal error bars indicate the estimated mass resolution. In the upper plot the colour-coded regions show the background expectation; in the lower plot the colour-coded regions show the event density expected from a SM Higgs boson ($m_H = 125$ GeV) (both in arbitrary units). (For interpretation of the references to colour in this figure legend, the reader is referred to the web version of this Letter.)

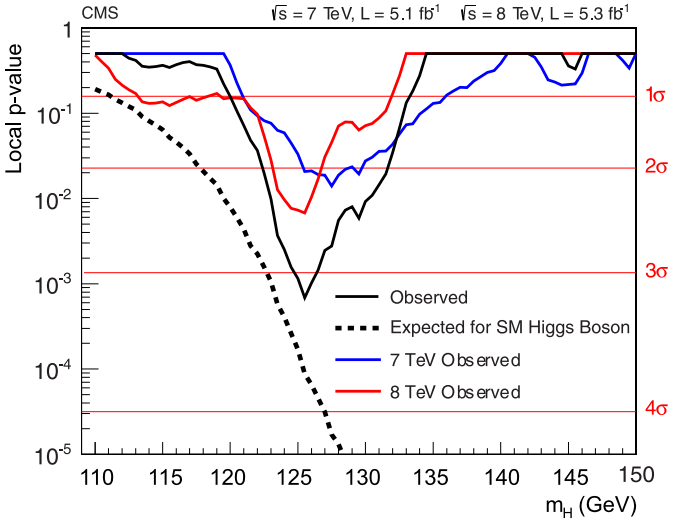

Fig. 6. The observed local p-value for the ZZ decay mode as a function of the SM Higgs boson mass. The dashed line shows the expected local p-values for a SM Higgs boson with a mass m_H.

data, falls steeply between 110 and 140 GeV, and has a value of 0.6 at $m_H = 125$ GeV. The observed upper limit indicates the presence of a significant excess in the range $120 < m_H < 130$ GeV. The local p-value is shown as a function of m_H in Fig. 6 for the 7 and 8 TeV data, and for their combination. The minimum local p-value in the data occurs at $m_H = 125.6$ GeV and has a significance of 3.2σ (expected 3.8σ). The combined best-fit signal strength for a SM Higgs boson mass hypothesis of 125.6 GeV is $\sigma/\sigma_{SM} = 0.7^{+0.4}_{-0.3}$.

6. Decay modes with low mass resolution

6.1. $H \to WW$

The decay mode $H \to WW$ is highly sensitive to a SM Higgs boson in the mass range around the WW threshold of 160 GeV. With the development of tools for lepton identification and E_T^{miss} reconstruction optimized for LHC pileup conditions, it is possible to extend the sensitivity down to 120 GeV. This decay mode is analysed by selecting events in which both W bosons decay leptonically, resulting in a signature with two isolated, oppositely charged leptons (electrons or muons) and large E_T^{miss} due to the undetected neutrinos [129,130]. A p_T threshold of 20 (10) GeV is applied to the lepton leading (subleading) in p_T. The analysis of the 7 TeV data is described in Ref. [26] and remains unchanged, while the 8 TeV analysis was modified to cope with more difficult conditions induced by the higher pileup of the 2012 data taking.

Events are classified according to the number of jets (0, 1, or 2) with $p_T > 30$ GeV and within $|\eta| < 4.7$ ($|\eta| < 5.0$ for the 7 TeV data set), and further separated into same-flavour (ee and $\mu\mu$) or different-flavour ($e\mu$) categories. Events with more than two jets are rejected. To improve the sensitivity of the analysis, the selection criteria are optimized separately for the different event categories since they are characterised by different dominating backgrounds. The zero-jet $e\mu$ category has the best signal sensitivity. Its main backgrounds are irreducible nonresonant WW production and reducible W + jets processes, where a jet is misidentified as a lepton. The one-jet $e\mu$ and zero-jet same-flavour categories only contribute to the signal sensitivity at the 10% level because of larger backgrounds, from top-quark decays and Drell–Yan production, respectively. Event selection in the two-jet category is optimized for the VBF production mechanism. This category has the highest expected signal-to-background ratio, but its contribution to the overall sensitivity is small owing to the lower cross section relative to inclusive production.

The projected E_T^{miss} variable [26] is used to reduce the Drell–Yan background arising from events where the E_T^{miss} vector is aligned with the lepton p_T, as well as events with mismeasured E_T^{miss} associated with poorly reconstructed leptons and jets. The projected E_T^{miss} is defined as the transverse component of the E_T^{miss} vector with respect to the closest lepton direction, if it is closer than $\pi/2$ in azimuthal angle, or the full E_T^{miss} otherwise. Since pileup degrades the projected E_T^{miss} resolution, the minimum of two different projected E_T^{miss} definitions is used: the first includes all particle candidates in the event, while the second uses only the charged particle candidates associated with the primary vertex. In the 8 TeV analysis, the minimum projected E_T^{miss} defined in this way is then required to be above a threshold that varies by category. For $m_H > 140$ GeV, projected E_T^{miss} is required to be greater than 20 GeV in the $e\mu$ channel, and greater than 45 GeV in the same-flavour channels. For $m_H \leqslant 140$ GeV in the same-flavour channels, where it is more difficult to separate the signal from the Drell–Yan background, a multivariate selection is used, combining kinematic and topological variables. In the two-jet category, a simple selection of $E_T^{miss} > 45$ GeV is applied. To further reduce the Drell–Yan background in the same-flavour final states, events with a dilepton mass within 15 GeV of the Z boson mass are rejected.

Table 4
Observed number of events, background estimates, and signal predictions for $m_H = 125$ GeV in each category of the WW analysis of the 8 TeV data set. All the selection requirements have been applied. The combined experimental and theoretical, systematic and statistical uncertainties are shown. The $Z\gamma$ process includes the dimuon, dielectron, and $\tau\tau \to \ell\ell$ final states.

Category:	0-jet eμ	0-jet $\ell\ell$	1-jet eμ	1-jet $\ell\ell$	2-jet eμ	2-jet $\ell\ell$
WW	87.6 ± 9.5	60.4 ± 6.7	19.5 ± 3.7	9.7 ± 1.9	0.4 ± 0.1	0.3 ± 0.1
WZ + ZZ + Zγ	2.2 ± 0.2	37.7 ± 12.5	2.4 ± 0.3	8.7 ± 4.9	0.1 ± 0.0	3.1 ± 1.8
Top	9.3 ± 2.7	1.9 ± 0.5	22.3 ± 2.0	9.5 ± 1.1	3.4 ± 1.9	2.0 ± 1.2
W + jets	19.1 ± 7.2	10.8 ± 4.3	11.7 ± 4.6	3.9 ± 1.7	0.3 ± 0.3	0.0 ± 0.0
W$\gamma^{(*)}$	6.0 ± 2.3	4.6 ± 2.5	5.9 ± 3.2	1.3 ± 1.2	0.0 ± 0.0	0.0 ± 0.0
All backgrounds	124.2 ± 12.4	115.5 ± 15.0	61.7 ± 7.0	33.1 ± 5.7	4.1 ± 1.9	5.4 ± 2.2
Signal ($m_H = 125$ GeV)	23.9 ± 5.2	14.9 ± 3.3	10.3 ± 3.0	4.4 ± 1.3	1.5 ± 0.2	0.8 ± 0.1
Data	158	123	54	43	6	7

The background from low-mass resonances is rejected by requiring a dilepton invariant mass greater than 12 GeV.

To suppress the top-quark background, a "top tagging" technique based on soft-muon and b-jet tagging is applied. The first method is designed to veto events containing muons in b jets coming from decays of top quarks. The second method uses a b-jet tagging algorithm, which looks within jets for tracks with large impact parameters. The algorithm is applied also in the case of zero-jet events, which may contain low-p_T jets below the selection threshold. To reduce the background from WZ production, events with a third lepton passing the identification and isolation requirements are rejected.

Yields for the dominant backgrounds are estimated using control regions in the data. The W + jets contribution is derived from data using a "tight–loose" sample in which one lepton passes the standard criteria and the other does not, but instead satisfies a "loose" set of requirements. The efficiency ϵ_{loose} for a jet that satisfies the loose selection to pass the tight selection is determined using data from an independent loose lepton-trigger sample dominated by jets. The background contamination is then estimated using the events of the "tight–loose" sample weighted by $\epsilon_{\text{loose}}/(1-\epsilon_{\text{loose}})$. The normalisation of the top-quark background is estimated by counting the number of top-tagged events and applying the corresponding top-tagging efficiency. The nonresonant WW contribution is normalised by using events with a dilepton mass larger than 100 GeV, where the Higgs boson signal contamination is negligible, extrapolated to the signal region using simulated samples. The same-flavour Drell–Yan background is normalised using the number of events observed with a dilepton mass within 7.5 GeV of the Z boson mass, after subtracting the non-Drell–Yan contribution. Other minor backgrounds from WZ, ZZ, and Wγ are estimated from simulation.

The 7 TeV data are analysed by training a BDT for each Higgs boson mass hypothesis in the zero-jet and one-jet event categories, while a simple selection strategy is employed in the VBF category [26]. In the BDT analysis, the Higgs boson signal is separated from the background by using a binned maximum-likelihood fit to the classifier distribution. The 8 TeV analysis is based on a simple selection strategy optimized for each mass hypothesis, where additional kinematic and topological requirements are applied to improve the signal-to-background ratio. One of the most sensitive variables to discriminate between $H \to WW$ decays and nonresonant WW production is the dilepton invariant mass $m_{\ell\ell}$. This quantity is shown in Fig. 7 for the zero-jet eμ category after the full selection for $m_H = 125$ GeV, except for the selection on $m_{\ell\ell}$ itself. Table 4 shows for the 8 TeV analysis the number of events selected in data, background estimates, and signal predictions for $m_H = 125$ GeV in each analysis category after applying all the selection requirements. About 97% of the signal events selected

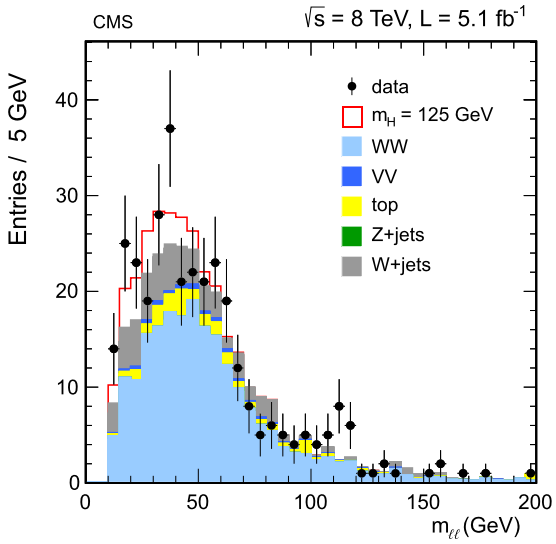

Fig. 7. Distribution of $m_{\ell\ell}$ for the zero-jet eμ category in the $H \to WW$ search at 8 TeV. The signal expected from a Higgs boson with a mass $m_H = 125$ GeV is shown added to the background.

in the zero-jet eμ category are expected to be produced by the gluon–gluon fusion process, whereas 83% of the signal in the two-jet eμ category is expected to be produced by the VBF process. The 95% CL expected and observed limits for the combination of the 7 and 8 TeV analyses are shown in Fig. 8. A broad excess is observed that is consistent with a SM Higgs boson of mass 125 GeV. This is illustrated by the dotted curve in Fig. 8 showing the median expected limit in the presence of a SM Higgs boson with $m_H = 125$ GeV. The expected significance for a SM Higgs of mass 125 GeV is 2.4σ and the observed significance is 1.6σ.

6.2. $H \to \tau\tau$

The decay mode $H \to \tau\tau$ is searched for in four exclusive subchannels, corresponding to different decays of the τ pair: eμ, $\mu\mu$, eτ_h, and $\mu\tau_h$, where electrons and muons arise from leptonic τ decays, and τ_h denotes hadronic τ decays. The latter are reconstructed by selecting τ decays consistent with the hypothesis of three charged pions, or one charged pion and up to two neutral pions [131]. The search is made in the mass range 110–145 GeV, and a signal should appear as a broad excess in the distribution of the τ-pair invariant mass $m_{\tau\tau}$.

The sensitivity of the search is improved by classifying the events according to jet multiplicity and the transverse momentum of the reconstructed τ. The multiplicity of jets with $p_T > 30$ GeV

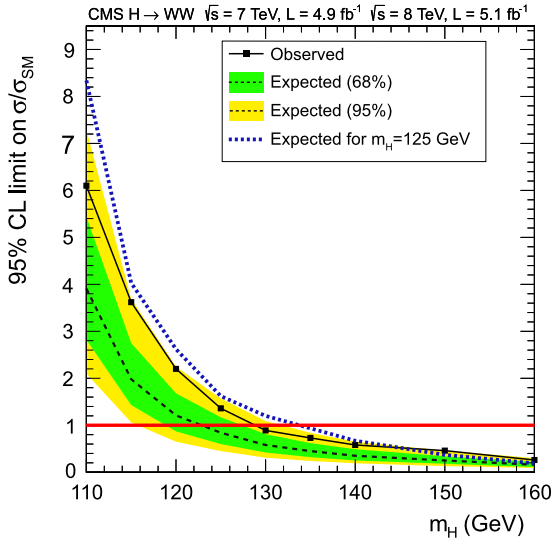

Fig. 8. The 95% CL limit on $\sigma/\sigma_{\mathrm{SM}}$ for a Higgs boson decaying, via a W boson pair, to two leptons and two neutrinos, for the combined 7 and 8 TeV data sets. The symbol $\sigma/\sigma_{\mathrm{SM}}$ denotes the production cross section times the relevant branching fractions, relative to the SM expectation. The background-only expectations are represented by their median (dashed line) and by the 68% and 95% CL bands. The dotted curve shows the median expected limit for a SM Higgs boson with $m_{\mathrm{H}} = 125$ GeV.

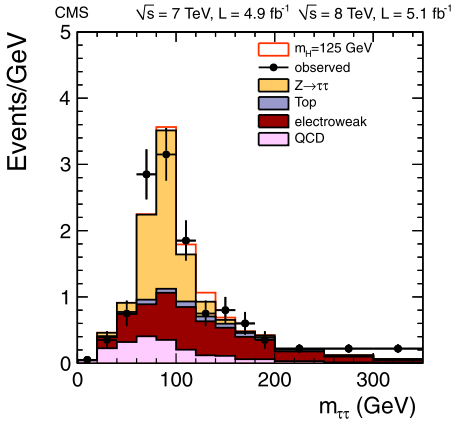

Fig. 9. Distribution of $m_{\tau\tau}$ in the combined 7 and 8 TeV data sets for the $\mu\tau_{\mathrm{h}}$ VBF category of the $\mathrm{H} \to \tau\tau$ search. The signal expected from a SM Higgs boson ($m_{\mathrm{H}} = 125$ GeV) is added to the background.

reflects the production mechanism: events with zero or one jet are likely to come from the gluon–gluon fusion process, while events with two jets are candidates for VBF production. Events including b jets with $p_{\mathrm{T}} > 20$ GeV are removed from zero- and one-jet categories. The signal purities in the zero- and one-jet categories are increased, and the $m_{\tau\tau}$ resolution is improved, by separating events into low- and high-p_{T} subchannels. The high-p_{T} subchannels are defined by $p_{\mathrm{T}}^{\tau_{\mathrm{h}}} > 40$ GeV in channels with a hadronic τ decay, and $p_{\mathrm{T}}^{\mu} > 35$ (30) GeV in the eμ ($\mu\mu$) channel. The mass $m_{\tau\tau}$ is reconstructed with an algorithm [132] combining the visible τ decay products and the missing transverse energy, achieving a resolution of about 20% on $m_{\tau\tau}$. Fig. 9 shows as an example the reconstructed $m_{\tau\tau}$ distribution in the $\mu\tau_{\mathrm{h}}$ VBF category for the combined 7 and 8 TeV data samples.

Backgrounds in the eμ and $\mu\mu$ channels arise from $\mathrm{t\bar{t}}$ and Drell–Yan production, while W and Z production with a misidentified τ_{h} candidate from an electron, muon, or jet dominates in the hadronic channels. Backgrounds from $\mathrm{Z} \to \tau\tau$ decays are modelled with $\mathrm{Z} \to \mu\mu$ events in data where each muon is replaced

Table 5
Numbers of expected and observed events in the most sensitive event categories (VBF) in the $\mathrm{H} \to \tau\tau$ analysis for the 7 and 8 TeV data sets. The expected signal yields for a SM Higgs boson with $m_{\mathrm{H}} = 125$ GeV are also shown. Combined statistical and systematic uncertainties in each estimate are reported.

Subchannel	eτ_{h}	$\mu\tau_{\mathrm{h}}$	eμ	$\mu\mu$
$\mathrm{Z} \to \tau\tau$	53 ± 5	100 ± 9	56 ± 12	5.3 ± 0.4
QCD	35 ± 7	41 ± 9	7.4 ± 1.4	–
W + jets	46 ± 10	72 ± 15	–	–
Z + jets	13 ± 2	2.5 ± 0.6	–	–
$\mathrm{Z} \to \mu\mu$	–	–	–	70 ± 8
$\mathrm{t\bar{t}}$	7.0 ± 1.7	14 ± 3	24 ± 2	6.7 ± 1.5
Dibosons	1.2 ± 0.9	2.9 ± 2.1	11 ± 2	2.4 ± 0.9
All backgrounds	156 ± 13	233 ± 20	99 ± 13	85 ± 9
Signal ($m_{\mathrm{H}} = 125$ GeV)	4.3 ± 0.6	7.7 ± 1.1	3.5 ± 0.4	0.8 ± 0.1
Data	142	263	110	83

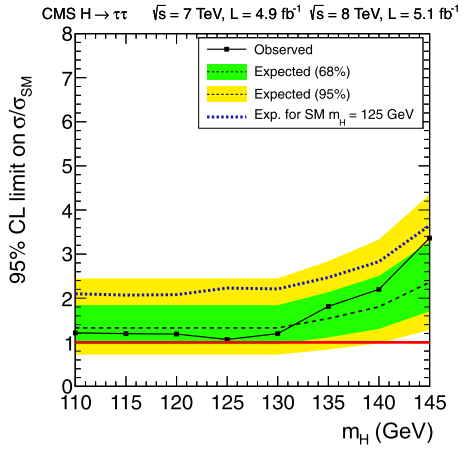

Fig. 10. The 95% CL limit on the signal strength $\sigma/\sigma_{\mathrm{SM}}$ for a Higgs boson decaying to τ pairs, for the combined 7 and 8 TeV data sets. The symbol $\sigma/\sigma_{\mathrm{SM}}$ denotes the production cross section times the relevant branching fractions, relative to the SM expectation. The background-only expectations are represented by their median (dashed line) and by the 68% and 95% CL bands. The dotted curve shows the median expected limit for a SM Higgs boson with $m_{\mathrm{H}} = 125$ GeV.

with particles from simulated decays of a τ with the same momentum as the muon. Reducible backgrounds, comprising W + jets, QCD multijet production, and residual $\mathrm{Z} \to$ ee events, are estimated from the data [27]. An improved signal-to-background ratio is achieved by including explicitly in the event selection for the VBF production mechanism the pseudorapidity separation between forward jets and the large invariant mass of the dijet system. Table 5 shows the numbers of expected and observed events in the most sensitive event categories (VBF) for the 7 and 8 TeV data sets. The expected signal yields for a SM Higgs boson with $m_{\mathrm{H}} = 125$ GeV are also shown.

To search for the presence of a Higgs boson signal in the selected events, a binned maximum-likelihood fit to $m_{\tau\tau}$ is performed jointly across the four final states, each with five event categories. Systematic uncertainties are represented by nuisance parameters in the fitting process. The expected and observed 95% CL limits on the signal strength for the combination of all categories are shown in Fig. 10. The expected and observed limits are 1.3 and 1.1 times the SM Higgs boson cross section at mass 125 GeV, respectively. The expected significance for a SM Higgs boson of mass 125 GeV is 1.4σ, and the observed value is zero.

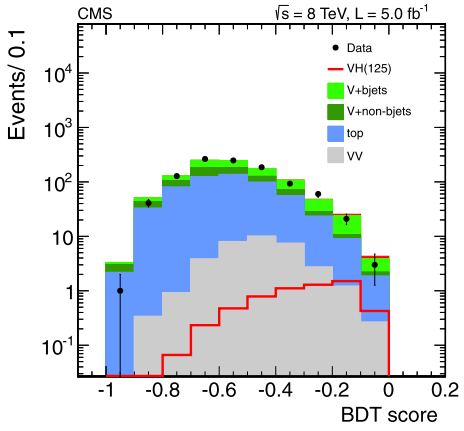

Fig. 11. Distribution of BDT scores for the high-p_T subchannel of the Z($\nu\nu$)H(bb) search in the 8 TeV data set after all selection criteria have been applied. The signal expected from a Higgs boson ($m_H = 125$ GeV), including W($\ell\nu$)H events where the charged lepton is not reconstructed, is shown added to the background and also overlaid for comparison with the diboson background.

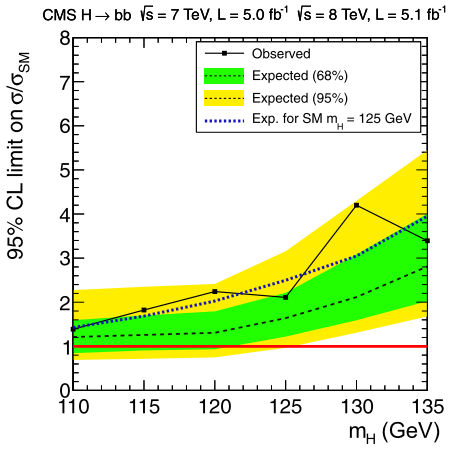

Fig. 12. The 95% CL limit on the signal strength σ/σ_{SM} for a Higgs boson decaying to two b quarks, for the combined 7 and 8 TeV data sets. The symbol σ/σ_{SM} denotes the production cross section times the relevant branching fractions, relative to the SM expectation. The background-only expectations are represented by their median (dashed line) and by the 68% and 95% CL bands. The dotted curve shows the median expected limit for a SM Higgs boson with $m_H = 125$ GeV.

6.3. H → bb

For $m_H \leqslant 135$ GeV, the decay H → bb has the largest branching fraction of the five search modes, but the inclusive signal is overwhelmed by QCD production of bottom quarks. The analysis is therefore designed to search for the associated production of the Higgs boson in events where a dijet resonance is produced at high p_T in association with a W or Z boson; this largely suppresses the QCD background. Five independent search channels are explored corresponding to different decays of the vector boson: Z($\ell\ell$)H, Z($\nu\nu$)H, and W($\ell\nu$)H. Events are further separated into two categories based on the p_T of the vector boson, ranging from 50–100 GeV for the lowest bin in the Z($\ell\ell$) search, to greater than 170 GeV for the highest bin in the W($\ell\nu$) search. For the Z($\nu\nu$) search, two subchannels are defined as $120 < E_T^{miss} < 160$ GeV and $E_T^{miss} > 160$ GeV. The two jets comprising the candidate Higgs boson decay are required to be identified as b jets, and the dijet system must satisfy a p_T threshold that is optimized within each channel: greater than 120 GeV for WH, 160 GeV for Z($\nu\nu$)H, and no explicit threshold for Z($\ell\ell$)H.

Dominant backgrounds arise from production of vector bosons in association with jets, pair- or single-production of top quarks, and diboson production (WW, WZ, ZZ) with one of the bosons decaying hadronically. Significant background rejection is achieved in general by requiring large p_T for the dijet, while also requiring that there be minimal additional jet activity and that the vector boson and dijet be back to back in azimuth. The effect on the signal efficiency of this selection due to higher-order electroweak [133] and QCD [91] corrections is accounted for in the systematic uncertainties. Further signal discrimination is obtained from the dijet invariant mass, which is expected to peak near m_H. A multivariate regression algorithm to better estimate b-jet p_T is trained on jets in simulated signal events and achieves a final dijet mass resolution of 8–9% for $m_H = 125$ GeV. The performance of the regression algorithm is checked in data using W/Z + jets and $t\bar{t}$ events.

A search for the signal is made in the distribution of scores of a BDT trained at discrete mass points. Input variables to the BDT algorithm exploit kinematic and topological information about the vector boson and dijet systems, and the colour-singlet nature of the Higgs boson [134]. The distribution of scores in simulated background events is checked using control regions in the data designed to enrich individual background contributions. Fig. 11 shows as an example the BDT scores for the high-p_T subchannel of the Z($\nu\nu$)H channel in the 8 TeV data set, after all selection criteria have been applied.

The rates for the dominant backgrounds arising from production of W/Z + jets and top-quark pairs are estimated in data [28], while contributions from single-top and diboson production are estimated from simulation studies. The signal is then searched for as an excess in the BDT score distribution using the predicted shapes for signal and background events, for Higgs boson masses in the range 110–135 GeV.

Combined results for expected and observed 95% CL limits obtained from the 7 and 8 TeV data sets are displayed in Fig. 12. The expected and observed limits are 1.6 and 2.1 times the SM Higgs boson cross section at mass 125 GeV. The expected local p-value for a SM Higgs of mass 125 GeV corresponds to 1.9σ, while the observed value corresponds to 0.7σ.

7. Combined results

The individual results for the channels analysed for the five decay modes, summarised in Table 1, are combined using the methods outlined in Section 4. The combination assumes the relative branching fractions predicted by the SM and takes into account the experimental statistical and systematic uncertainties as well as the theoretical uncertainties, which are dominated by the imperfect knowledge of the QCD scale and parton distribution functions. The CL_s is shown in Fig. 13 as a function of the Higgs boson mass hypothesis. The observed values are shown by the solid points. The dashed line indicates the median of the expected results for the background-only hypothesis, with the green (dark) and yellow (light) bands indicating the ranges in which the CL_s values are expected to lie in 68% and 95% of the experiments under the background-only hypothesis. The probabilities for an observation, in the absence of a signal, to lie above or below the 68% (95%) band are 16% (2.5%) each. The thick horizontal lines indicate CL_s values of 0.05, 0.01, and 0.001. The mass regions where the observed CL_s values are below these lines are excluded with the corresponding $(1 - CL_s)$ confidence levels. Our previously published results exclude the SM Higgs boson from 127 to 600 GeV [21]. In the search described here, the SM Higgs boson is excluded at 95% CL in the range $110 < m_H < 121.5$ GeV. In the range $121.5 < m_H < 128$ GeV a significant excess is seen and the SM Higgs boson cannot be excluded at 95% CL.

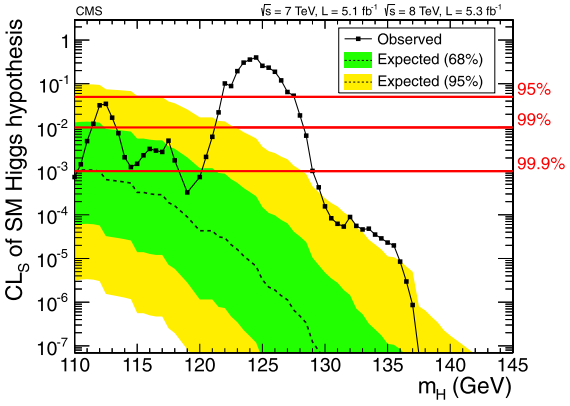

Fig. 13. The CL_s values for the SM Higgs boson hypothesis as a function of the Higgs boson mass in the range 110–145 GeV. The background-only expectations are represented by their median (dashed line) and by the 68% and 95% CL bands. (For interpretation of the references to colour, the reader is referred to the web version of this Letter.)

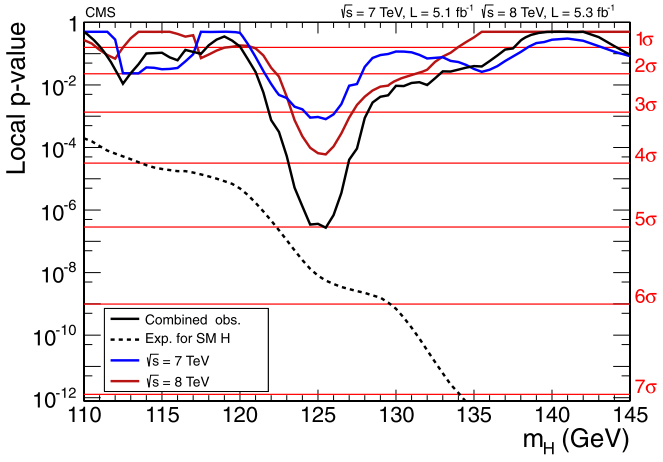

Fig. 14. The observed local p-value for 7 TeV and 8 TeV data, and their combination as a function of the SM Higgs boson mass. The dashed line shows the expected local p-values for a SM Higgs boson with a mass m_H.

7.1. Significance of the observed excess

The consistency of the observed excess with the background-only hypothesis may be judged from Fig. 14, which shows a scan of the local p-value for the 7 and 8 TeV data sets and their combination. The 7 and 8 TeV data sets exhibit an excess of 3.2σ and 3.8σ significance, respectively, for a Higgs boson mass of approximately 125 GeV. In the overall combination the significance is 5.0σ for $m_H = 125.5$ GeV. Fig. 15 gives the local p-value for the five decay modes individually and displays the expected overall p-value.

The largest contributors to the overall excess in the combination are the $\gamma\gamma$ and ZZ decay modes. They both have very good mass resolution, allowing good localization of the invariant mass of a putative resonance responsible for the excess. Their combined significance reaches 5.0σ (Fig. 16). The WW decay mode has an exclusion sensitivity comparable to the $\gamma\gamma$ and ZZ decay modes but does not have a good mass resolution. It has an excess with local significance 1.6σ for $m_H \sim 125$ GeV. When added to the $\gamma\gamma$ and ZZ decay modes, the combined significance becomes 5.1σ. Adding the $\tau\tau$ and bb channels in the combination, the final significance becomes 5.0σ. Table 6 summarises the expected and observed local p-values for a SM Higgs boson mass hypothesis of 125.5 GeV for the various combinations of channels.

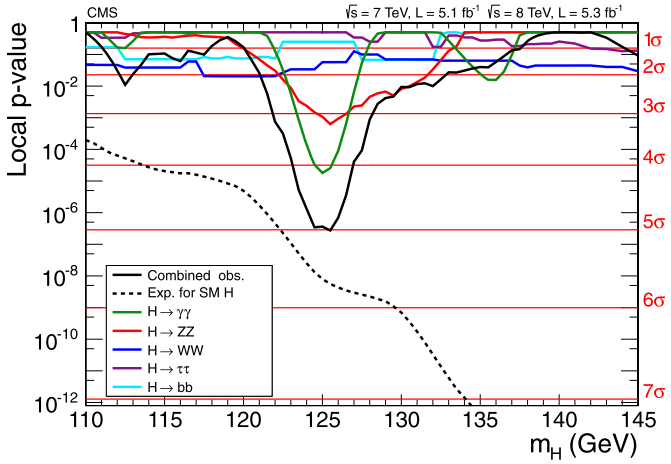

Fig. 15. The observed local p-value for the five decay modes and the overall combination as a function of the SM Higgs boson mass. The dashed line shows the expected local p-values for a SM Higgs boson with a mass m_H.

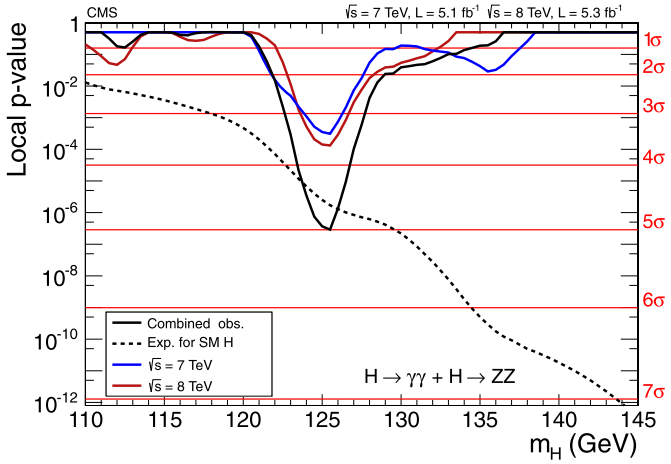

Fig. 16. The observed local p-value for decay modes with high mass-resolution channels, $\gamma\gamma$ and ZZ, as a function of the SM Higgs boson mass. The dashed line shows the expected local p-values for a SM Higgs boson with a mass m_H.

Table 6
The expected and observed local p-values, expressed as the corresponding number of standard deviations of the observed excess from the background-only hypothesis, for $m_H = 125.5$ GeV, for various combinations of decay modes.

Decay mode/combination	Expected (σ)	Observed (σ)
$\gamma\gamma$	2.8	4.1
ZZ	3.8	3.2
$\tau\tau + \mathrm{bb}$	2.4	0.5
$\gamma\gamma + \mathrm{ZZ}$	4.7	5.0
$\gamma\gamma + \mathrm{ZZ} + \mathrm{WW}$	5.2	5.1
$\gamma\gamma + \mathrm{ZZ} + \mathrm{WW} + \tau\tau + \mathrm{bb}$	5.8	5.0

The global p-value for the search range 115–130 (110–145) GeV is calculated using the method suggested in Ref. [115], and corresponds to 4.6σ (4.5σ). These results confirm the very low probability for an excess as large as or larger than that observed to arise from a statistical fluctuation of the background. The excess constitutes the observation of a new particle with a mass near 125 GeV, manifesting itself in decays to two photons or to ZZ. These two decay modes indicate that the new particle is a boson; the two-photon decay implies that its spin is different from one [135,136].

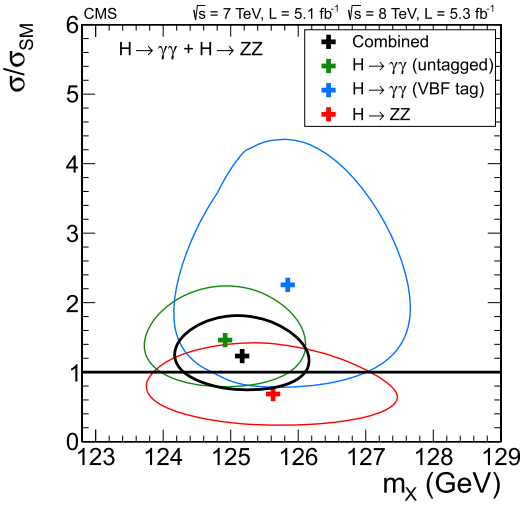

Fig. 17. The 68% CL contours for the signal strength σ/σ_{SM} versus the boson mass m_X for the untagged $\gamma\gamma$, $\gamma\gamma$ with VBF-like dijet, 4ℓ, and their combination. The symbol σ/σ_{SM} denotes the production cross section times the relevant branching fractions, relative to the SM expectation. In this combination, the relative signal strengths for the three decay modes are constrained by the expectations for the SM Higgs boson.

7.2. Mass of the observed boson

The mass m_X of the observed boson is determined using the $\gamma\gamma$ and ZZ decay modes, with the former dominating the precision of the measurement. The calibration of the energy scale in the $\gamma\gamma$ decay mode is achieved with reference to the known Z boson mass, as described in Section 5.1. There are two main sources of systematic uncertainty: (i) imperfect simulation of the differences between electrons and photons and (ii) the need to extrapolate from m_Z to $m_X \approx 125$ GeV. The systematic uncertainties are evaluated by making comparisons between data and simulated samples of $Z \to ee$ and $H \to \gamma\gamma$ ($m_H = 90$ GeV). The two uncertainties, which together amount to 0.5%, are assumed to be fully correlated between all the $\gamma\gamma$ event categories in the 7 and 8 TeV data. For the $ZZ \to 4\ell$ decay mode the energy scale (for electrons) and momentum scale (for muons) are calibrated using the leptonic decays of the Z boson, with an assigned uncertainty of 0.4%.

Fig. 17 shows the two-dimensional 68% CL regions for the signal strength σ/σ_{SM} versus m_X for the three channels (untagged $\gamma\gamma$, dijet-tagged $\gamma\gamma$, and $ZZ \to 4\ell$). The combined 68% CL contour shown in Fig. 17 assumes that the relative event yields among the three channels are those expected from the standard model, while the overall signal strength is a free parameter.

To extract the value of m_X in a model-independent way, the signal yields of the three channels are allowed to vary independently. Thus the expected event yields in these channels are scaled by independent factors, while the signal is assumed to be due to a particle with a unique mass m_X. The combined best-fit mass is $m_X = 125.3 \pm 0.4(\text{stat.}) \pm 0.5(\text{syst.})$ GeV.

7.3. Compatibility with the SM Higgs boson hypothesis

A first test of the compatibility of the observed boson with the SM Higgs boson is provided by examination of the best-fit value for the common signal strength σ/σ_{SM}, obtained in a combination of all search channels. Fig. 18 shows a scan of the overall σ/σ_{SM} obtained in the combination of all channels versus a hypothesised Higgs boson mass m_H. The band corresponds to the $\pm 1\sigma$ uncertainty (statistical and systematic). The excesses seen in the 7 TeV and 8 TeV data, and in their combination, around 125 GeV are

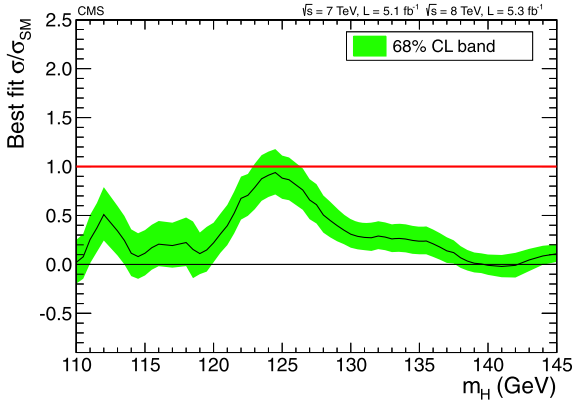

Fig. 18. The observed best-fit signal strength σ/σ_{SM} as a function of the SM Higgs boson mass in the range 110–145 GeV for the combined 7 and 8 TeV data sets. The symbol σ/σ_{SM} denotes the production cross section times the relevant branching fractions, relative to the SM expectation. The band corresponds to the ± 1 standard deviation uncertainty in σ/σ_{SM}.

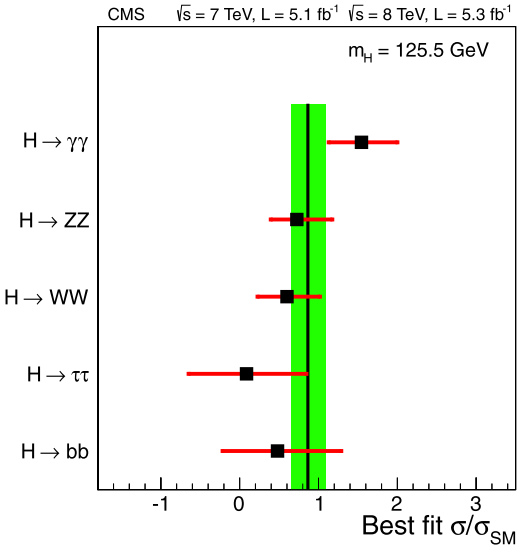

Fig. 19. Values of σ/σ_{SM} for the combination (solid vertical line) and for individual decay modes (points). The vertical band shows the overall σ/σ_{SM} value 0.87 ± 0.23. The symbol σ/σ_{SM} denotes the production cross section times the relevant branching fractions, relative to the SM expectation. The horizontal bars indicate the ± 1 standard deviation uncertainties in the σ/σ_{SM} values for individual modes; they include both statistical and systematic uncertainties.

consistent with unity within the $\pm 1\sigma$ uncertainties. The observed σ/σ_{SM} value for an excess at 125.5 GeV in a combination of all data is 0.87 ± 0.23. The different decay channels and data sets have been examined for self-consistency. Fig. 19 shows the measured values of σ/σ_{SM} results obtained for the different decay modes. These results are consistent, within uncertainties, with the expectations for the SM Higgs boson.

8. Conclusions

Results are presented from searches for the standard model Higgs boson in proton–proton collisions at $\sqrt{s} = 7$ and 8 TeV in the CMS experiment at the LHC, using data samples corresponding to integrated luminosities of up to 5.1 fb^{-1} at 7 TeV and 5.3 fb^{-1} at 8 TeV. The search is performed in five decay modes: $\gamma\gamma$, ZZ, W^+W^-, $\tau^+\tau^-$, and $b\bar{b}$. An excess of events is observed above the expected background, with a local significance of 5.0σ, at a mass near 125 GeV, signalling the production of a new par-

ticle. The expected local significance for a standard model Higgs boson of that mass is 5.8σ. The global p-value in the search range of 115–130 (110–145) GeV corresponds to 4.6σ (4.5σ). The excess is most significant in the two decay modes with the best mass resolution, $\gamma\gamma$ and ZZ, and a fit to these signals gives a mass of $125.3 \pm 0.4(\text{stat.}) \pm 0.5(\text{syst.})$ GeV. The decay to two photons indicates that the new particle is a boson with spin different from one. The results presented here are consistent, within uncertainties, with expectations for the standard model Higgs boson. The collection of further data will enable a more rigorous test of this conclusion and an investigation of whether the properties of the new particle imply physics beyond the standard model.

Acknowledgements

We congratulate our colleagues in the CERN accelerator departments for the excellent performance of the LHC machine. We thank the computing centres in the Worldwide LHC computing Grid for the provisioning and excellent performance of computing infrastructure essential to our analyses. We gratefully acknowledge the contributions of the technical staff at CERN and other CMS institutes. We also thank the administrative staff at CERN and the other CMS institutes and acknowledge support from BMWF and FWF (Austria); FNRS and FWO (Belgium); CNPq, CAPES, FAPERJ, and FAPESP (Brazil); MES (Bulgaria); CERN; CAS, MoST, and NSFC (China); COLCIENCIAS (Colombia); MSES (Croatia); RPF (Cyprus); MEYS (Czech Republic); MoER, SF0690030s09 and ERDF (Estonia); Academy of Finland, MEC, and HIP (Finland); CEA and CNRS/IN2P3 (France); BMBF, DFG, and HGF (Germany); GSRT (Greece); OTKA and NKTH (Hungary); DAE and DST (India); IPM (Iran); SFI (Ireland); INFN (Italy); NRF and WCU (Republic of Korea); LAS (Lithuania); CINVESTAV, CONACYT, SEP, and UASLP-FAI (Mexico); MSI (New Zealand); PAEC (Pakistan); MSHE and NSC (Poland); FCT (Portugal); JINR (Armenia, Belarus, Georgia, Ukraine, Uzbekistan); MON, RosAtom, RAS and RFBR (Russia); MSTD (Serbia); SEIDI and CPAN (Spain); Swiss Funding Agencies (Switzerland); NSC (Taipei); TUBITAK and TAEK (Turkey); NASU (Ukraine); STFC (United Kingdom); DOE and NSF (USA). Individuals have received support from the Marie-Curie programme and the European Research Council (European Union); the Leventis Foundation; the A.P. Sloan Foundation; the Alexander von Humboldt Foundation; the Austrian Science Fund (FWF); the Belgian Federal Science Policy Office; the Fonds pour la Formation à la Recherche dans l'Industrie et dans l'Agriculture (FRIA-Belgium); the Agentschap voor Innovatie door Wetenschap en Technologie (IWT-Belgium); the Council of Science and Industrial Research, India; the Compagnia di San Paolo (Torino); and the HOMING PLUS programme of Foundation for Polish Science, cofinanced from European Union, Regional Development Fund.

Open access

References

[1] F. Englert, R. Brout, Phys. Rev. Lett. 13 (1964) 321, http://dx.doi.org/10.1103/PhysRevLett.13.321.
[2] P.W. Higgs, Phys. Lett. 12 (1964) 132, http://dx.doi.org/10.1016/0031-9163(64)91136-9.
[3] P.W. Higgs, Phys. Rev. Lett. 13 (1964) 508, http://dx.doi.org/10.1103/PhysRevLett.13.508.
[4] G.S. Guralnik, C.R. Hagen, T.W.B. Kibble, Phys. Rev. Lett. 13 (1964) 585, http://dx.doi.org/10.1103/PhysRevLett.13.585.
[5] P.W. Higgs, Phys. Rev. 145 (1966) 1156, http://dx.doi.org/10.1103/PhysRev.145.1156.
[6] T.W.B. Kibble, Phys. Rev. 155 (1967) 1554, http://dx.doi.org/10.1103/PhysRev.155.1554.
[7] S.L. Glashow, Nucl. Phys. 22 (1961) 579, http://dx.doi.org/10.1016/0029-5582(61)90469-2.
[8] S. Weinberg, Phys. Rev. Lett. 19 (1967) 1264, http://dx.doi.org/10.1103/PhysRevLett.19.1264.
[9] A. Salam, in: N. Svartholm (Ed.), Elementary Particle Physics: Relativistic Groups and Analyticity, Almqvist & Wiskell, 1968, p. 367, proceedings of the eighth Nobel symposium.
[10] J.M. Cornwall, D.N. Levin, G. Tiktopoulos, Phys. Rev. Lett. 30 (1973) 1268, http://dx.doi.org/10.1103/PhysRevLett.30.1268.
[11] J.M. Cornwall, D.N. Levin, G. Tiktopoulos, Phys. Rev. D 10 (1974) 1145, http://dx.doi.org/10.1103/PhysRevD.10.1145, also Erratum, http://dx.doi.org/10.1103/PhysRevD.11.972.
[12] C.H. Llewellyn Smith, Phys. Lett. B 46 (1973) 233, http://dx.doi.org/10.1016/0370-2693(73)90692-8.
[13] B.W. Lee, C. Quigg, H.B. Thacker, Phys. Rev. D 16 (1977) 1519, http://dx.doi.org/10.1103/PhysRevD.16.1519.
[14] ALEPH, CDF, D0, DELPHI, L3, OPAL, SLD Collaborations, the LEP Electroweak Working Group, the Tevatron Electroweak Working Group, and the SLD Electroweak and Heavy Flavour Groups, Precision electroweak measurements and constraints on the standard model, CERN PH-EP-2010-095, at this time, the most up-to-date Higgs boson mass constraints come from http://lepewwg.web.cern.ch/LEPEWWG/plots/winter2012/, arXiv:1012.2367, 2010, http://cdsweb.cern.ch/record/1313716.
[15] ALEPH, DELPHI, L3, OPAL Collaborations, and LEP Working Group for Higgs Boson Searches, Phys. Lett. B 565 (2003) 61, arXiv:hep-ex/0306033, http://dx.doi.org/10.1016/S0370-2693(03)00614-2.
[16] CDF and D0 Collaborations, Phys. Rev. Lett. 104 (2010) 061802, http://dx.doi.org/10.1103/PhysRevLett.104.061802.
[17] CDF Collaboration, Phys. Rev. Lett. (2012), submitted for publication, arXiv:1207.1707.
[18] CDF and D0 Collaborations, Phys. Rev. Lett. 109 (2012) 071804, http://dx.doi.org/10.1103/PhysRevLett.109.071804.
[19] D0 Collaboration, Phys. Rev. Lett. (2012), submitted for publication, arXiv:1207.6631.
[20] L. Evans, P. Bryant (Eds.), LHC Machine, JINST 3 (2008) S08001, http://dx.doi.org/10.1088/1748-0221/3/08/S08001.
[21] S. Chatrchyan, et al., Phys. Lett. B 710 (2012) 26, arXiv:1202.1488, http://dx.doi.org/10.1016/j.physletb.2012.02.064.
[22] G. Aad, et al., Phys. Rev. D 86 (2012) 032003, arXiv:1207.0319, http://dx.doi.org/10.1103/PhysRevD.86.032003.
[23] LHC Higgs Cross Section Working Group, in: S. Dittmaier, C. Mariotti, G. Passarino, R. Tanaka (Eds.), Handbook of LHC Higgs Cross Sections: 1. Inclusive Observables, CERN, Geneva, 2011, arXiv:1101.0593, http://cdsweb.cern.ch/record/1318996.
[24] S. Chatrchyan, et al., Phys. Lett. B 710 (2012) 403, arXiv:1202.1487, http://dx.doi.org/10.1016/j.physletb.2012.03.003.
[25] S. Chatrchyan, et al., Phys. Rev. Lett. 108 (2012) 111804, arXiv:1202.1997, http://dx.doi.org/10.1103/PhysRevLett.108.111804.
[26] S. Chatrchyan, et al., Phys. Lett. B 710 (2012) 91, arXiv:1202.1489, http://dx.doi.org/10.1016/j.physletb.2012.02.076.
[27] S. Chatrchyan, et al., Phys. Lett. B 713 (2012) 68, arXiv:1202.4083, http://dx.doi.org/10.1016/j.physletb.2012.05.028.
[28] S. Chatrchyan, et al., Phys. Lett. B 710 (2012) 284, arXiv:1202.4195, http://dx.doi.org/10.1016/j.physletb.2012.02.085.
[29] M. Della Negra, et al., in: G. Jarlskog, D. Rein (Eds.), Proceedings of the Large Hadron Collider Workshop, Aachen, Germany, 1990, p. 467, CERN 90-10-V-3/ECFA 90-133-V-3, http://cdsweb.cern.ch/record/215299/files/CERN-90-10-V-3.pdf.
[30] M. Della Negra, et al., Letter of intent by the CMS Collaboration for a general purpose detector at the LHC, Tech. Rep. CERN-LHCC-92-03, CERN-LHCC-I-1, CERN, 1992, https://cdsweb.cern.ch/record/290808.
[31] N. Ellis, T.S. Virdee, Ann. Rev. Nucl. Part. Sci. 44 (1994) 609, http://dx.doi.org/10.1146/annurev.ns.44.120194.003141.
[32] S. Chatrchyan, et al., The CMS experiment at the CERN LHC, JINST 3 (2008) S08004, http://dx.doi.org/10.1088/1748-0221/3/08/S08004.
[33] CMS Collaboration, b-jet identification in the CMS experiment, CMS Physics Analysis Summary CMS-PAS-BTV-11-004, 2012, https://cdsweb.cern.ch/record/1427247.
[34] V. Khachatryan, et al., Phys. Rev. D 83 (2011) 112004, arXiv:1012.5545, http://dx.doi.org/10.1103/PhysRevD.83.112004.
[35] CMS Collaboration, Particle-flow event reconstruction in CMS and performance for jets, taus, and $E_{\mathrm{T}}^{\mathrm{miss}}$, CMS Physics Analysis Summary CMS-PAS-PFT-09-001, 2009, http://cdsweb.cern.ch/record/1194487.

[36] CMS Collaboration, Commissioning of the particle-flow event reconstruction with the first LHC collisions recorded in the CMS detector, CMS Physics Analysis Summary CMS-PAS-PFT-10-001, 2010, http://cdsweb.cern.ch/record/1247373.

[37] M. Cacciari, G.P. Salam, G. Soyez, JHEP 0804 (2008) 063, http://dx.doi.org/10.1088/1126-6708/2008/04/063.

[38] M. Cacciari, G.P. Salam, Phys. Lett. B 659 (2008) 119, http://dx.doi.org/10.1016/j.physletb.2007.09.077.

[39] M. Cacciari, G.P. Salam, G. Soyez, JHEP 0804 (2008) 005, http://dx.doi.org/10.1088/1126-6708/2008/04/005.

[40] M. Cacciari, G.P. Salam, G. Soyez, Eur. Phys. J. C 72 (2012) 1896, arXiv:1111.6097, http://dx.doi.org/10.1140/epjc/s10052-012-1896-2.

[41] S. Chatrchyan, et al., JINST 6 (2011) 11002, arXiv:1107.4277, http://dx.doi.org/10.1088/1748-0221/6/11/P11002.

[42] S. Chatrchyan, et al., JINST 6 (2011) 9001, arXiv:1106.5048, http://dx.doi.org/10.1088/1748-0221/6/09/P09001.

[43] CMS Collaboration, Commissioning of the particle-flow event reconstruction with leptons from J/ψ and W decays at 7 TeV, CMS Physics Analysis Summary CMS-PAS-PFT-10-003, 2010, http://cdsweb.cern.ch/record/1279347.

[44] CMS Collaboration, Electron reconstruction and identification at $\sqrt{s} = 7$ TeV, CMS Physics Analysis Summary CMS-PAS-EGM-10-004, 2010, http://cdsweb.cern.ch/record/1299116.

[45] S. Baffioni, C. Charlot, F. Ferri, D. Futyan, P. Meridiani, et al., Eur. Phys. J. C 49 (2007) 1099, http://dx.doi.org/10.1140/epjc/s10052-006-0175-5.

[46] W. Adam, R. Fruhwirth, A. Strandlie, T. Todorov, J. Phys. G 31 (2005) N9, http://dx.doi.org/10.1088/0954-3899/31/9/N01.

[47] CMS Collaboration, Absolute calibration of the luminosity measurement at CMS: Winter 2012 update, CMS Physics Analysis Summary CMS-PAS-SMP-12-008, 2012, https://cdsweb.cern.ch/record/1434360.

[48] S. van der Meer, Calibration of the effective beam height in the ISR, Tech. Rep. CERN-ISR-PO-68-31, CERN, Geneva, 1968, https://cdsweb.cern.ch/record/296752.

[49] J.R. Ellis, M.K. Gaillard, D.V. Nanopoulos, Nucl. Phys. B 106 (1976) 292, http://dx.doi.org/10.1016/0550-3213(76)90382-5.

[50] H.M. Georgi, S.L. Glashow, M.E. Machacek, D.V. Nanopoulos, Phys. Rev. Lett. 40 (1978) 692, http://dx.doi.org/10.1103/PhysRevLett.40.692.

[51] S.L. Glashow, D.V. Nanopoulos, A. Yildiz, Phys. Rev. D 18 (1978) 1724, http://dx.doi.org/10.1103/PhysRevD.18.1724.

[52] R.N. Cahn, S.D. Ellis, R. Kleiss, W.J. Stirling, Phys. Rev. D 35 (1987) 1626, http://dx.doi.org/10.1103/PhysRevD.35.1626.

[53] J.F. Gunion, G.L. Kane, J. Wudka, Nucl. Phys. B 299 (1988) 231, http://dx.doi.org/10.1016/0550-3213(88)90284-2.

[54] D.L. Rainwater, D. Zeppenfeld, JHEP 9712 (1997) 005, arXiv:hep-ph/9712271, http://dx.doi.org/10.1088/1126-6708/1997/12/005.

[55] D.L. Rainwater, D. Zeppenfeld, K. Hagiwara, Phys. Rev. D 59 (1998) 014037, arXiv:hep-ph/9808468, http://dx.doi.org/10.1103/PhysRevD.59.014037.

[56] D.L. Rainwater, D. Zeppenfeld, Phys. Rev. D 60 (1999) 113004, arXiv:hep-ph/9906218, http://dx.doi.org/10.1103/PhysRevD.60.113004, also Erratum, http://dx.doi.org/10.1103/PhysRevD.61.099901.

[57] A. Djouadi, M. Spira, P.M. Zerwas, Phys. Lett. B 264 (1991) 440, http://dx.doi.org/10.1016/0370-2693(91)90375-Z.

[58] S. Dawson, Nucl. Phys. B 359 (1991) 283, http://dx.doi.org/10.1016/0550-3213(91)90061-2.

[59] M. Spira, A. Djouadi, D. Graudenz, P.M. Zerwas, Nucl. Phys. B 453 (1995) 17, arXiv:hep-ph/9504378, http://dx.doi.org/10.1016/0550-3213(95)00379-7.

[60] R.V. Harlander, W.B. Kilgore, Phys. Rev. Lett. 88 (2002) 201801, arXiv:hep-ph/0201206, http://dx.doi.org/10.1103/PhysRevLett.88.201801.

[61] C. Anastasiou, K. Melnikov, Nucl. Phys. B 646 (2002) 220, arXiv:hep-ph/0207004, http://dx.doi.org/10.1016/S0550-3213(02)00837-4.

[62] V. Ravindran, J. Smith, W.L. van Neerven, Nucl. Phys. B 665 (2003) 325, arXiv:hep-ph/0302135, http://dx.doi.org/10.1016/S0550-3213(03)00457-7.

[63] S. Catani, D. de Florian, M. Grazzini, P. Nason, JHEP 0307 (2003) 028, http://dx.doi.org/10.1088/1126-6708/2003/07/028.

[64] U. Aglietti, R. Bonciani, G. Degrassi, A. Vicini, Phys. Lett. B 595 (2004) 432, arXiv:hep-ph/0404071, http://dx.doi.org/10.1016/j.physletb.2004.06.063.

[65] G. Degrassi, F. Maltoni, Phys. Lett. B 600 (2004) 255, arXiv:hep-ph/0407249, http://dx.doi.org/10.1016/j.physletb.2004.09.008.

[66] S. Actis, G. Passarino, C. Sturm, S. Uccirati, Phys. Lett. B 670 (2008) 12, arXiv:0809.1301, http://dx.doi.org/10.1016/j.physletb.2008.10.018.

[67] C. Anastasiou, R. Boughezal, F. Petriello, JHEP 0904 (2009) 003, arXiv:0811.3458, http://dx.doi.org/10.1088/1126-6708/2009/04/003.

[68] D. de Florian, M. Grazzini, Phys. Lett. B 674 (2009) 291, arXiv:0901.2427, http://dx.doi.org/10.1016/j.physletb.2009.03.033.

[69] J. Baglio, A. Djouadi, JHEP 1103 (2011) 055, arXiv:1012.0530, http://dx.doi.org/10.1007/JHEP03(2011)055.

[70] D. de Florian, M. Grazzini, Higgs production at the LHC: updated cross sections at $\sqrt{s} = 8$ TeV, arXiv:1206.4133, 2012.

[71] G. Bozzi, S. Catani, D. de Florian, M. Grazzini, Nucl. Phys. B 737 (2006) 73, arXiv:hep-ph/0508068, http://dx.doi.org/10.1016/j.nuclphysb.2005.12.022.

[72] D. de Florian, G. Ferrera, M. Grazzini, D. Tommasini, JHEP 1111 (2011) 064, http://dx.doi.org/10.1007/JHEP11(2011)064.

[73] G. Passarino, C. Sturm, S. Uccirati, Nucl. Phys. B 834 (2010) 77, arXiv:1001.3360, http://dx.doi.org/10.1016/j.nuclphysb.2010.03.013.

[74] I.W. Stewart, F.J. Tackmann, Phys. Rev. D 85 (2012) 034011, arXiv:1107.2117, http://dx.doi.org/10.1103/PhysRevD.85.034011.

[75] A. Djouadi, J. Kalinowski, M. Spira, Comput. Phys. Commun. 108 (1998) 56, arXiv:hep-ph/9704448, http://dx.doi.org/10.1016/S0010-4655(97)00123-9.

[76] A. Djouadi, J. Kalinowski, M. Muhlleitner, M. Spira, in: The Les Houches 2009 workshop on TeV colliders: The tools and Monte Carlo working group summary report, arXiv:1003.1643, 2010.

[77] A. Bredenstein, A. Denner, S. Dittmaier, M.M. Weber, Phys. Rev. D 74 (2006) 013004, arXiv:hep-ph/0604011, http://dx.doi.org/10.1103/PhysRevD.74.013004.

[78] A. Bredenstein, A. Denner, S. Dittmaier, M.M. Weber, JHEP 0702 (2007) 080, arXiv:hep-ph/0611234, http://dx.doi.org/10.1088/1126-6708/2007/02/080.

[79] S. Actis, G. Passarino, C. Sturm, S. Uccirati, Nucl. Phys. B 811 (2009) 182, arXiv:0809.3667, http://dx.doi.org/10.1016/j.nuclphysb.2008.11.024.

[80] A. Denner, S. Heinemeyer, I. Puljak, D. Rebuzzi, M. Spira, Eur. Phys. J. C 71 (2011) 1753, arXiv:1107.5909, http://dx.doi.org/10.1140/epjc/s10052-011-1753-8.

[81] M. Ciccolini, A. Denner, S. Dittmaier, Phys. Rev. Lett. 99 (2007) 161803, arXiv:0707.0381, http://dx.doi.org/10.1103/PhysRevLett.99.161803.

[82] M. Ciccolini, A. Denner, S. Dittmaier, Phys. Rev. D 77 (2008) 013002, arXiv:0710.4749, http://dx.doi.org/10.1103/PhysRevD.77.013002.

[83] T. Figy, C. Oleari, D. Zeppenfeld, Phys. Rev. D 68 (2003) 073005, arXiv:hep-ph/0306109, http://dx.doi.org/10.1103/PhysRevD.68.073005.

[84] K. Arnold, M. Bahr, G. Bozzi, F. Campanario, C. Englert, et al., Comput. Phys. Commun. 180 (2009) 1661, arXiv:0811.4559, http://dx.doi.org/10.1016/j.cpc.2009.03.006.

[85] P. Bolzoni, F. Maltoni, S.-O. Moch, M. Zaro, Phys. Rev. Lett. 105 (2010) 011801, arXiv:1003.4451, http://dx.doi.org/10.1103/PhysRevLett.105.011801.

[86] T. Han, S. Willenbrock, Phys. Lett. B 273 (1991) 167, http://dx.doi.org/10.1016/0370-2693(91)90572-8.

[87] O. Brein, A. Djouadi, R. Harlander, Phys. Lett. B 579 (2004) 149, arXiv:hep-ph/0307206, http://dx.doi.org/10.1016/j.physletb.2003.10.112.

[88] M.L. Ciccolini, S. Dittmaier, M. Krämer, Phys. Rev. D 68 (2003) 073003, arXiv:hep-ph/0306234, http://dx.doi.org/10.1103/PhysRevD.68.073003.

[89] R. Hamberg, W.L. van Neerven, T. Matsuura, Nucl. Phys. B 359 (1991) 343, http://dx.doi.org/10.1016/0550-3213(91)90064-5.

[90] A. Denner, S. Dittmaier, S. Kallweit, A. Muck, EW corrections to Higgs strahlung at the Tevatron and the LHC with HAWK, arXiv:1112.5258, 2011.

[91] G. Ferrera, M. Grazzini, F. Tramontano, Phys. Rev. Lett. 107 (2011) 152003, arXiv:1107.1164, http://dx.doi.org/10.1103/PhysRevLett.107.152003.

[92] W. Beenakker, S. Dittmaier, M. Kramer, B. Plumper, M. Spira, et al., Phys. Rev. Lett. 87 (2001) 201805, arXiv:hep-ph/0107081, http://dx.doi.org/10.1103/PhysRevLett.87.201805.

[93] W. Beenakker, S. Dittmaier, M. Kramer, B. Plumper, M. Spira, et al., Nucl. Phys. B 653 (2003) 151, arXiv:hep-ph/0211352, http://dx.doi.org/10.1016/S0550-3213(03)00044-0.

[94] S. Dawson, L.H. Orr, L. Reina, D. Wackeroth, Phys. Rev. D 67 (2003) 071503, arXiv:hep-ph/0211438, http://dx.doi.org/10.1103/PhysRevD.67.071503.

[95] S. Dawson, C. Jackson, L.H. Orr, L. Reina, D. Wackeroth, Phys. Rev. D 68 (2003) 034022, arXiv:hep-ph/0305087, http://dx.doi.org/10.1103/PhysRevD.68.034022.

[96] M. Botje, J. Butterworth, A. Cooper-Sarkar, A. de Roeck, J. Feltesse, et al., The PDF4LHC Working Group interim recommendations, arXiv:1101.0538, 2011.

[97] S. Alekhin, S. Alioli, R.D. Ball, V. Bertone, J. Blumlein, et al., The PDF4LHC Working Group interim report, arXiv:1101.0536, 2011.

[98] H.-L. Lai, M. Guzzi, J. Huston, Z. Li, P.M. Nadolsky, et al., Phys. Rev. D 82 (2010) 074024, arXiv:1007.2241, http://dx.doi.org/10.1103/PhysRevD.82.074024.

[99] A.D. Martin, W.J. Stirling, R.S. Thorne, G. Watt, Eur. Phys. J. C 63 (2009) 189, arXiv:0901.0002, http://dx.doi.org/10.1140/epjc/s10052-009-1072-5.

[100] R.D. Ball, et al., Nucl. Phys. B 849 (2011) 296, arXiv:1101.1300, http://dx.doi.org/10.1016/j.nuclphysb.2011.03.021.

[101] C. Anastasiou, S. Buehler, F. Herzog, A. Lazopoulos, JHEP 1204 (2012) 004, arXiv:1202.3638, http://dx.doi.org/10.1007/JHEP04(2012)004.

[102] LHC Higgs Cross Section Working Group, in: S. Dittmaier, C. Mariotti, G. Passarino, R. Tanaka (Eds.), Handbook of LHC Higgs Cross Sections: 2. Differential Distributions, CERN, Geneva, 2012, arXiv:1201.3084.

[103] S. Agostinelli, et al., Nucl. Instrum. Meth. A 506 (2003) 250, http://dx.doi.org/10.1016/S0168-9002(03)01368-8.

[104] S. Alioli, P. Nason, C. Oleari, E. Re, JHEP 0904 (2009) 002, http://dx.doi.org/10.1088/1126-6708/2009/04/002.

[105] P. Nason, C. Oleari, JHEP 1002 (2010) 037, http://dx.doi.org/10.1007/JHEP02(2010)037.

[106] T. Sjöstrand, S. Mrenna, P.Z. Skands, JHEP 0605 (2006) 026, http://dx.doi.org/10.1088/1126-6708/2006/05/026.

[107] G. Bozzi, S. Catani, D. de Florian, M. Grazzini, Phys. Lett. B 564 (2003) 65, http://dx.doi.org/10.1016/S0370-2693(03)00656-7.

[108] C. Anastasiou, K. Melnikov, F. Petriello, Nucl. Phys. B 724 (2005) 197, http://dx.doi.org/10.1016/j.nuclphysb.2005.06.036.
[109] C. Anastasiou, S. Bucherer, Z. Kunszt, JHEP 0910 (2009) 068, http://dx.doi.org/10.1088/1126-6708/2009/10/068.
[110] S. Gieseke, D. Grellscheid, K. Hamilton, A. Ribon, P. Richardson, et al., Herwig++ 2.0 Release Note, arXiv:hep-ph/0609306, 2006.
[111] J. Alwall, P. Demin, S. de Visscher, R. Frederix, M. Herquet, et al., JHEP 0709 (2007) 028, arXiv:0706.2334, http://dx.doi.org/10.1088/1126-6708/2007/09/028.
[112] ATLAS and CMS Collaborations, LHC Higgs Combination Group, Procedure for the LHC Higgs boson search combination in Summer 2011, Tech. Rep. ATL-PHYS-PUB 2011-11, CMS NOTE 2011/005, 2011, http://cdsweb.cern.ch/record/1379837.
[113] T. Junk, Nucl. Instrum. Meth. A 434 (1999) 435, http://dx.doi.org/10.1016/S0168-9002(99)00498-2.
[114] A.L. Read, J. Phys. G 28 (2002) 2693, http://dx.doi.org/10.1088/0954-3899/28/10/313.
[115] E. Gross, O. Vitells, Eur. Phys. J. C 70 (2010) 525, arXiv:1005.1891, http://dx.doi.org/10.1140/epjc/s10052-010-1470-8.
[116] G. Cowan, K. Cranmer, E. Gross, O. Vitells, Eur. Phys. J. C 71 (2011) 1554, arXiv:1007.1727, http://dx.doi.org/10.1140/epjc/s10052-011-1554-0.
[117] L. Moneta, K. Belasco, K. Cranmer, S. Kreiss, et al., in: 13th Int. Workshop on Advanced Computing and Analysis Techniques in Physics Research (ACAT2010), 2010, PoS ACAT:057, arXiv:1009.1003, http://pos.sissa.it/archive/conferences/093/057/ACAT2010_057.pdf.
[118] C.J. Seez, T.S. Virdee, L. Di Lella, R.H. Kleiss, Z. Kunszt, W.J. Stirling, in: G. Jarlskog, D. Rein (Eds.), Proceedings of the Large Hadron Collider Workshop, Aachen, Germany, 1990, p. 474, CERN 90-10-V-2/ECFA 90-133-V-2, http://cdsweb.cern.ch/record/220524.
[119] B.P. Roe, H.-J. Yang, J. Zhu, Y. Liu, I. Stancu, et al., Nucl. Instrum. Meth. A 543 (2005) 577, http://dx.doi.org/10.1016/j.nima.2004.12.018.
[120] H. Voss, A. Höcker, J. Stelzer, F. Tegenfeldt, in: XI Int. Workshop on Advanced Computing and Analysis Techniques in Physics Research, 2007, PoS ACAT:040, arXiv:physics/0703039, http://pos.sissa.it/archive/conferences/050/040/ACAT_040.pdf.
[121] R.J. Barlow, J. Comp. Phys. 72 (1987) 202, http://dx.doi.org/10.1016/0021-9991(87)90078-7.
[122] M. Della Negra, D. Froidevaux, K. Jakobs, R. Kinnunen, R. Kleiss, A. Nisati, T. Sjöstrand, in: G. Jarlskog, D. Rein (Eds.), Proceedings of the Large Hadron Collider Workshop, Aachen, Germany, 1990, p. 509, CERN 90-10-V-2/ECFA 90-133-V-2, http://cdsweb.cern.ch/record/215298.
[123] N. Cabibbo, A. Maksymowicz, Phys. Rev. B 137 (1965) 438, http://dx.doi.org/10.1103/PhysRev.137.B438, also Erratum, http://dx.doi.org/10.1103/PhysRev.168.1926.
[124] Y. Gao, A.V. Gritsan, Z. Guo, K. Melnikov, M. Schulze, et al., Phys. Rev. D 81 (2010) 075022, arXiv:1001.3396, http://dx.doi.org/10.1103/PhysRevD.81.075022.
[125] A. De Rujula, J. Lykken, M. Pierini, C. Rogan, M. Spiropulu, Phys. Rev. D 82 (2010) 013003, arXiv:1001.5300, http://dx.doi.org/10.1103/PhysRevD.82.013003.
[126] S. Chatrchyan, et al., JHEP 1204 (2012) 036, arXiv:1202.1416, http://dx.doi.org/10.1007/JHEP04(2012)036.
[127] S.Y. Choi, D.J. Miller, M.M. Muhlleitner, P.M. Zerwas, Phys. Lett. B 553 (2003) 61, arXiv:hep-ph/0210077, http://dx.doi.org/10.1016/S0370-2693(02)03191-X.
[128] S. Chatrchyan, et al., JHEP 1110 (2011) 132, http://dx.doi.org/10.1007/JHEP10(2011)132.
[129] V.D. Barger, G. Bhattacharya, T. Han, B.A. Kniehl, Phys. Rev. D 43 (1991) 779, http://dx.doi.org/10.1103/PhysRevD.43.779.
[130] M. Dittmar, H.K. Dreiner, Phys. Rev. D 55 (1997) 167, arXiv:hep-ph/9608317, http://dx.doi.org/10.1103/PhysRevD.55.167.
[131] S. Chatrchyan, et al., JINST 7 (2011) P01001, http://dx.doi.org/10.1088/1748-0221/7/01/P01001.
[132] S. Chatrchyan, et al., Phys. Rev. Lett. 106 (2011) 231801, arXiv:1104.1619, http://dx.doi.org/10.1103/PhysRevLett.106.231801.
[133] A. Denner, S. Dittmaier, S. Kallweit, A. Muck, JHEP 1203 (2012) 075, arXiv:1112.5142, http://dx.doi.org/10.1007/JHEP03(2012)075.
[134] J. Gallicchio, M.D. Schwartz, Phys. Rev. Lett. 105 (2010) 022001, arXiv:1001.5027, http://dx.doi.org/10.1103/PhysRevLett.105.022001.
[135] L.D. Landau, Dokl. Akad. Nauk 60 (1948) 207.
[136] C.N. Yang, Phys. Rev. 77 (1950) 242, http://dx.doi.org/10.1103/PhysRev.77.242.

CMS Collaboration

S. Chatrchyan, V. Khachatryan, A.M. Sirunyan, A. Tumasyan

Yerevan Physics Institute, Yerevan, Armenia

W. Adam, E. Aguilo, T. Bergauer, M. Dragicevic, J. Erö, C. Fabjan [1], M. Friedl, R. Frühwirth [1], V.M. Ghete, J. Hammer, M. Hoch, N. Hörmann, J. Hrubec, M. Jeitler [1], W. Kiesenhofer, V. Knünz, M. Krammer [1], I. Krätschmer, D. Liko, W. Majerotto, I. Mikulec, M. Pernicka [†], B. Rahbaran, C. Rohringer, H. Rohringer, R. Schöfbeck, J. Strauss, F. Szoncsó, A. Taurok, W. Waltenberger, G. Walzel, E. Widl, C.-E. Wulz [1]

Institut für Hochenergiephysik der OeAW, Wien, Austria

V. Chekhovsky, I. Emeliantchik, A. Litomin, V. Makarenko, V. Mossolov, N. Shumeiko, A. Solin, R. Stefanovitch, J. Suarez Gonzalez

National Centre for Particle and High Energy Physics, Minsk, Belarus

A. Fedorov, M. Korzhik, O. Missevitch, R. Zuyeuski

Research Institute for Nuclear Problems, Minsk, Belarus

M. Bansal, S. Bansal, W. Beaumont, T. Cornelis, E.A. De Wolf, D. Druzhkin, X. Janssen, S. Luyckx, L. Mucibello, S. Ochesanu, B. Roland, R. Rougny, M. Selvaggi, Z. Staykova, H. Van Haevermaet, P. Van Mechelen, N. Van Remortel, A. Van Spilbeeck

Universiteit Antwerpen, Antwerpen, Belgium

F. Blekman, S. Blyweert, J. D'Hondt, O. Devroede, R. Gonzalez Suarez, R. Goorens, A. Kalogeropoulos, M. Maes, A. Olbrechts, S. Tavernier, W. Van Doninck, L. Van Lancker, P. Van Mulders, G.P. Van Onsem, I. Villella

Vrije Universiteit Brussel, Brussel, Belgium

B. Clerbaux, G. De Lentdecker, V. Dero, J.P. Dewulf, A.P.R. Gay, T. Hreus, A. Léonard, P.E. Marage, A. Mohammadi, T. Reis, S. Rugovac, L. Thomas, C. Vander Velde, P. Vanlaer, J. Wang, J. Wickens

Université Libre de Bruxelles, Bruxelles, Belgium

V. Adler, K. Beernaert, A. Cimmino, S. Costantini, G. Garcia, M. Grunewald, B. Klein, J. Lellouch, A. Marinov, J. Mccartin, A.A. Ocampo Rios, D. Ryckbosch, N. Strobbe, F. Thyssen, M. Tytgat, S. Walsh, E. Yazgan, N. Zaganidis

Ghent University, Ghent, Belgium

S. Basegmez, G. Bruno, R. Castello, L. Ceard, J. De Favereau De Jeneret, C. Delaere, P. Demin, T. du Pree, D. Favart, L. Forthomme, A. Giammanco [2], G. Grégoire, J. Hollar, V. Lemaitre, J. Liao, O. Militaru, C. Nuttens, D. Pagano, A. Pin, K. Piotrzkowski, N. Schul, J.M. Vizan Garcia

Université Catholique de Louvain, Louvain-la-Neuve, Belgium

N. Beliy, T. Caebergs, E. Daubie, G.H. Hammad

Université de Mons, Mons, Belgium

G.A. Alves, L. Brito, M. Correa Martin Junior, T. Martins, M.E. Pol, M.H.G. Souza

Centro Brasileiro de Pesquisas Fisicas, Rio de Janeiro, Brazil

W.L. Aldá Júnior, W. Carvalho, A. Custódio, E.M. Da Costa, D. De Jesus Damiao, C. De Oliveira Martins, S. Fonseca De Souza, D. Matos Figueiredo, L. Mundim, H. Nogima, V. Oguri, W.L. Prado Da Silva, A. Santoro, A. Sznajder, A. Vilela Pereira

Universidade do Estado do Rio de Janeiro, Rio de Janeiro, Brazil

T.S. Anjos [3], C.A. Bernardes [3], F.A. Dias [4], T.R. Fernandez Perez Tomei, E.M. Gregores [3], R.L. Iope, C. Lagana, S.M. Lietti, F. Marinho, P.G. Mercadante [3], S.F. Novaes, Sandra S. Padula

Instituto de Fisica Teorica, Universidade Estadual Paulista, Sao Paulo, Brazil

L. Dimitrov, V. Genchev [5], P. Iaydjiev [5], S. Piperov, M. Rodozov, S. Stoykova, G. Sultanov, V. Tcholakov, R. Trayanov, I. Vankov, M. Vutova

Institute for Nuclear Research and Nuclear Energy, Sofia, Bulgaria

C. Roumenin, D. Uzunova, R. Zahariev

Institute of System Engineering and Robotics, Sofia, Bulgaria

A. Dimitrov, R. Hadjiiska, V. Kozhuharov, L. Litov, B. Pavlov, P. Petkov

University of Sofia, Sofia, Bulgaria

J.G. Bian, G.M. Chen, H.S. Chen, K.L. He, C.H. Jiang, W.G. Li, D. Liang, S. Liang, X. Meng, G. Sun, H.S. Sun, J. Tao, J. Wang, X. Wang, Z. Wang, H. Xiao, M. Xu, M. Yang, J. Zang, X. Zhang, Z. Zhang, Z. Zhang, W.R. Zhao, Z. Zhu

Institute of High Energy Physics, Beijing, China

C. Asawatangtrakuldee, Y. Ban, J. Cai, S. Guo, Y. Guo, W. Li, H.T. Liu, S. Liu, Y. Mao, S.J. Qian, H. Teng, D. Wang, Y.L. Ye, L. Zhang, B. Zhu, W. Zou

State Key Lab. of Nucl. Phys. and Tech., Peking University, Beijing, China

C. Avila, J.P. Gomez, B. Gomez Moreno, A.F. Osorio Oliveros, J.C. Sanabria

Universidad de Los Andes, Bogota, Colombia

N. Godinovic, D. Lelas, R. Plestina [6], D. Polic, I. Puljak [5]

Technical University of Split, Split, Croatia

Z. Antunovic, M. Kovac

University of Split, Split, Croatia

V. Brigljevic, S. Duric, K. Kadija, J. Luetic, S. Morovic

Institute Rudjer Boskovic, Zagreb, Croatia

A. Attikis, M. Galanti, G. Mavromanolakis, J. Mousa, C. Nicolaou, F. Ptochos, P.A. Razis

University of Cyprus, Nicosia, Cyprus

M. Finger, M. Finger Jr.

Charles University, Prague, Czech Republic

A. Aly, Y. Assran [7], A. Awad, S. Elgammal [8], A. Ellithi Kamel [9], S. Khalil [8], M.A. Mahmoud [10], A. Mahrous, A. Radi [11,12]

Academy of Scientific Research and Technology of the Arab Republic of Egypt, Egyptian Network of High Energy Physics, Cairo, Egypt

A. Hektor, M. Kadastik, K. Kannike, M. Müntel, M. Raidal, L. Rebane, A. Strumia, A. Tiko

National Institute of Chemical Physics and Biophysics, Tallinn, Estonia

P. Eerola, G. Fedi, M. Voutilainen

Department of Physics, University of Helsinki, Helsinki, Finland

E. Anttila, J. Härkönen, A. Heikkinen, V. Karimäki, H.M. Katajisto, R. Kinnunen, M.J. Kortelainen, M. Kotamäki, T. Lampén, K. Lassila-Perini, S. Lehti, T. Lindén, P. Luukka, T. Mäenpää, T. Peltola, E. Tuominen, J. Tuominiemi, E. Tuovinen, D. Ungaro, T.P. Vanhala, L. Wendland

Helsinki Institute of Physics, Helsinki, Finland

K. Banzuzi, A. Karjalainen, A. Korpela, T. Tuuva

Lappeenranta University of Technology, Lappeenranta, Finland

M. Anfreville, M. Besancon, S. Choudhury, M. Dejardin, D. Denegri, B. Fabbro, J.L. Faure, F. Ferri, S. Ganjour, F.X. Gentit, A. Givernaud, P. Gras, G. Hamel de Monchenault, P. Jarry, F. Kircher, M.C. Lemaire, E. Locci, J. Malcles, I. Mandjavidze, A. Nayak, J.P. Pansart, J. Rander, J.M. Reymond, A. Rosowsky, I. Shreyber, M. Titov, P. Verrecchia

DSM/IRFU, CEA/Saclay, Gif-sur-Yvette, France

J. Badier, S. Baffioni, F. Beaudette, E. Becheva, L. Benhabib, L. Bianchini, M. Bluj [13], C. Broutin, P. Busson, M. Cerutti, D. Chamont, C. Charlot, N. Daci, T. Dahms, M. Dalchenko, L. Dobrzynski, Y. Geerebaert, R. Granier de Cassagnac, M. Haguenauer, P. Hennion, G. Milleret, P. Miné, C. Mironov, I.N. Naranjo, M. Nguyen, C. Ochando, P. Paganini, T. Romanteau, D. Sabes, R. Salerno, A. Sartirana, Y. Sirois, C. Thiebaux, C. Veelken, A. Zabi

Laboratoire Leprince-Ringuet, Ecole Polytechnique, IN2P3–CNRS, Palaiseau, France

J.-L. Agram [14], J. Andrea, A. Besson, D. Bloch, D. Bodin, J.-M. Brom, M. Cardaci, E.C. Chabert, C. Collard, E. Conte [14], F. Drouhin [14], C. Ferro, J.-C. Fontaine [14], D. Gelé, U. Goerlach, C. Goetzmann, L. Gross, D. Huss, P. Juillot, E. Kieffer, A.-C. Le Bihan, J. Pansanel, Y. Patois, P. Van Hove

Institut Pluridisciplinaire Hubert Curien, Université de Strasbourg, Université de Haute Alsace Mulhouse, CNRS/IN2P3, Strasbourg, France

D. Boutigny, D. Mercier

Centre de Calcul de l'Institut National de Physique Nucleaire et de Physique des Particules, CNRS/IN2P3, Villeurbanne, France, Villeurbanne, France

G. Baulieu, S. Beauceron, N. Beaupere, M. Bedjidian, O. Bondu, G. Boudoul, S. Brochet, J. Chasserat, R. Chierici [5], C. Combaret, D. Contardo, P. Depasse, H. El Mamouni, J. Fay, S. Gascon, N. Giraud, M. Gouzevitch, R. Haroutunian, B. Ille, T. Kurca, M. Lethuillier, N. Lumb, H. Mathez, L. Mirabito, S. Perries, L. Sgandurra, V. Sordini, Y. Tschudi, M. Vander Donckt, P. Verdier, S. Viret

Université de Lyon, Université Claude Bernard Lyon 1, CNRS–IN2P3, Institut de Physique Nucléaire de Lyon, Villeurbanne, France

V. Roinishvili, L. Rurua

E. Andronikashvili Institute of Physics, Academy of Science, Tbilisi, Georgia

N. Amaglobeli, I. Bagaturia, B. Chiladze, R. Kvatadze, D. Lomidze, R. Shanidze, Z. Tsamalaidze [15]

Institute of High Energy Physics and Informatization, Tbilisi State University, Tbilisi, Georgia

R. Adolphi, G. Anagnostou, C. Autermann, S. Beranek, R. Brauer, W. Braunschweig, B. Calpas, M. Edelhoff, L. Feld, N. Heracleous, O. Hindrichs, R. Jussen, W. Karpinski, K. Klein, K. Lübelsmeyer, J. Merz, A. Ostapchuk, D. Pandoulas, A. Perieanu, F. Raupach, J. Sammet, S. Schael, D. Schmitz, A. Schultz von Dratzig, R. Siedling, D. Sprenger, H. Weber, B. Wittmer, M. Wlochal, V. Zhukov [16]

RWTH Aachen University, I. Physikalisches Institut, Aachen, Germany

M. Ata, P. Biallass, J. Caudron, E. Dietz-Laursonn, D. Duchardt, M. Erdmann, R. Fischer, A. Güth, T. Hebbeker, C. Heidemann, G. Hilgers, K. Hoepfner, C. Hof, T. Klimkovich, D. Klingebiel, P. Kreuzer, C. Magass, M. Merschmeyer, A. Meyer, M. Olschewski, P. Papacz, B. Philipps, H. Pieta, H. Reithler, S.A. Schmitz, L. Sonnenschein, M. Sowa, J. Steggemann, D. Teyssier, M. Weber

RWTH Aachen University, III. Physikalisches Institut A, Aachen, Germany

M. Bontenackels, V. Cherepanov, Y. Erdogan, G. Flügge, H. Geenen, M. Geisler, W. Haj Ahmad, F. Hoehle, B. Kargoll, T. Kress, Y. Kuessel, J. Lingemann [5], A. Nowack, L. Perchalla, O. Pooth, P. Sauerland, A. Stahl, M.H. Zoeller

RWTH Aachen University, III. Physikalisches Institut B, Aachen, Germany

M. Aldaya Martin, J. Behr, W. Behrenhoff, U. Behrens, M. Bergholz [17], A. Bethani, K. Borras, A. Burgmeier, A. Cakir, L. Calligaris, A. Campbell, E. Castro, F. Costanza, D. Dammann, C. Diez Pardos, G. Eckerlin, D. Eckstein, A. Flossdorf, G. Flucke, A. Geiser, I. Glushkov, P. Goettlicher, A. Grebenyuk, P. Gunnellini, S. Habib, J. Hauk, G. Hellwig, H. Jung, M. Kasemann, P. Katsas, C. Kleinwort, H. Kluge, A. Knutsson, M. Krämer, D. Krücker, E. Kuznetsova, W. Lange, B. Lewendel, W. Lohmann [17], B. Lutz, R. Mankel, I. Marfin, M. Marienfeld, I.-A. Melzer-Pellmann, A.B. Meyer, J. Mnich, C. Muhl, A. Mussgiller, S. Naumann-Emme, O. Novgorodova, J. Olzem, A. Parenti, H. Perrey, A. Petrukhin, D. Pitzl, A. Raspereza, P.M. Ribeiro Cipriano, C. Riedl, E. Ron, C. Rosemann, M. Rosin, J. Salfeld-Nebgen, R. Schmidt [17], T. Schoerner-Sadenius, N. Sen, A. Spiridonov, M. Stein, J. Tomaszewska, D. Volyanskyy, R. Walsh, C. Wissing, C. Youngman

Deutsches Elektronen-Synchrotron, Hamburg, Germany

V. Blobel, J. Draeger, H. Enderle, J. Erfle, U. Gebbert, M. Görner, T. Hermanns, R.S. Höing, K. Kaschube, G. Kaussen, H. Kirschenmann, R. Klanner, J. Lange, B. Mura, F. Nowak, T. Peiffer, N. Pietsch, D. Rathjens, C. Sander, H. Schettler, P. Schleper, E. Schlieckau, A. Schmidt, M. Schröder, T. Schum, M. Seidel, J. Sibille [18], V. Sola, H. Stadie, G. Steinbrück, J. Thomsen, L. Vanelderen

University of Hamburg, Hamburg, Germany

C. Barth, J. Bauer, J. Berger, P. Blüm, C. Böser, V. Buege, Z.Y. Chen, S. Chowdhury, T. Chwalek, D. Daeuwel, W. De Boer, A. Descroix, A. Dierlamm, G. Dirkes, M. Fahrer, M. Feindt, U. Felzmann, M. Frey, A. Furgeri,

I. Gebauer, A. Gessler, J. Gruschke, M. Guthoff [5], C. Hackstein, F. Hartmann, F. Hauler, T. Hauth [5], S. Heier, S.M. Heindl, M. Heinrich, A. Heiss, H. Held, K.H. Hoffmann, S. Honc, U. Husemann, M. Imhof, C. Jung, S. Junghans, I. Katkov [16], U. Kerzel, D. Knoblauch, J.R. Komaragiri, M. Kräber, T. Kuhr, T. Liamsuwan, P. Lobelle Pardo, D. Martschei, A. Menchikov, X. Mol, D. Mörmann, S. Mueller, Th. Müller, D. Neuberger, M.B. Neuland, M. Niegel, A. Nürnberg, O. Oberst, A. Oehler, T. Ortega Gomez, J. Ott, C. Piasecki, A. Poschlad, G. Quast, K. Rabbertz, F. Ratnikov, N. Ratnikova, M. Renz, S. Röcker, F. Roederer, A. Sabellek, C. Saout, A. Scheurer, D. Schieferdecker, P. Schieferdecker, F.-P. Schilling, M. Schmanau, G. Schott, W. Schwerdtfeger, H.J. Simonis, A. Skiba, F.M. Stober, A. Theel, W.H. Thümmel, D. Troendle, A. Trunov, R. Ulrich, J. Wagner-Kuhr, S. Wayand, M. Weber, T. Weiler, M. Zeise, E.B. Ziebarth, M. Zvada

Institut für Experimentelle Kernphysik, Karlsruhe, Germany

G. Daskalakis, T. Geralis, S. Kesisoglou, A. Kyriakis, D. Loukas, I. Manolakos, A. Markou, C. Markou, C. Mavrommatis, E. Ntomari

Institute of Nuclear Physics "Demokritos", Aghia Paraskevi, Greece

L. Gouskos, A. Panagiotou, N. Saoulidou

University of Athens, Athens, Greece

I. Evangelou, C. Foudas, P. Kokkas, N. Manthos, I. Papadopoulos, V. Patras, F.A. Triantis

University of Ioánnina, Ioánnina, Greece

G. Bencze, C. Hajdu, P. Hidas, D. Horvath [19], F. Sikler, V. Veszpremi, G. Vesztergombi [20], P. Zalan

KFKI Research Institute for Particle and Nuclear Physics, Budapest, Hungary

N. Beni, S. Czellar, A. Fenyvesi, J. Molnar, J. Palinkas, Z. Szillasi

Institute of Nuclear Research ATOMKI, Debrecen, Hungary

J. Karancsi, P. Raics, Z.L. Trocsanyi, B. Ujvari, G. Zilizi

University of Debrecen, Debrecen, Hungary

S.B. Beri, V. Bhandari, V. Bhatnagar, N. Dhingra, R. Gupta, M. Kaur, J.M. Kohli, M.Z. Mehta, N. Nishu, L.K. Saini, A. Sharma, J.B. Singh

Panjab University, Chandigarh, India

Ashok Kumar, Arun Kumar, S. Ahuja, A. Bhardwaj, S. Chatterji, B.C. Choudhary, P. Gupta, S. Malhotra, M. Naimuddin, K. Ranjan, V. Sharma, R.K. Shivpuri

University of Delhi, Delhi, India

S. Banerjee, S. Bhattacharya, S. Dutta, B. Gomber, Sa. Jain, Sh. Jain, R. Khurana, S. Sarkar, M. Sharan

Saha Institute of Nuclear Physics, Kolkata, India

A. Abdulsalam, R.K. Choudhury, D. Dutta, M. Ghodgaonkar, S. Kailas, S.K. Kataria, V. Kumar, P. Mehta, A.K. Mohanty [5], L.M. Pant, P. Shukla, A. Topkar

Bhabha Atomic Research Centre, Mumbai, India

T. Aziz, S. Chendvankar, P.V. Deshpande, S.N. Ganguli, S. Ganguly, M. Guchait [21], A. Gurtu [22], M. Maity [23], K. Mazumdar, G.B. Mohanty, B. Parida, M.R. Patil, R. Raghavan, K. Sudhakar, N. Wickramage

Tata Institute of Fundamental Research – EHEP, Mumbai, India

B.S. Acharya, S. Banerjee, S. Bheesette, S. Dugad, S.D. Kalmani, M.R. Krishnaswamy, V.R. Lakkireddi, N.K. Mondal, V.S. Narasimham, N. Panyam, P. Verma

Tata Institute of Fundamental Research – HECR, Mumbai, India

F. Ardalan, H. Arfaei [24], H. Bakhshiansohi, S.M. Etesami [25], A. Fahim [24], M. Hashemi, A. Jafari, M. Khakzad, M. Mohammadi Najafabadi, S. Paktinat Mehdiabadi, B. Safarzadeh [26], M. Zeinali

Institute for Research in Fundamental Sciences (IPM), Tehran, Iran

M. Abbrescia [a,b], L. Barbone [a,b], C. Calabria [a,b,5], S.S. Chhibra [a,b], A. Colaleo [a], D. Creanza [a,c], N. De Filippis [a,c,5], M. De Palma [a,b], G. De Robertis [a], G. Donvito [a], L. Fiore [a], G. Iaselli [a,c], F. Loddo [a], G. Maggi [a,c], M. Maggi [a], N. Manna [a,b], B. Marangelli [a,b], S. My [a,c], S. Natali [a,b], S. Nuzzo [a,b], N. Pacifico [a], A. Pompili [a,b], G. Pugliese [a,c], A. Ranieri [a], F. Romano [a,c], G. Selvaggi [a,b], L. Silvestris [a], G. Singh [a,b], V. Spinoso [a], R. Venditti [a,b], P. Verwilligen, G. Zito [a]

[a] *INFN Sezione di Bari, Bari, Italy*
[b] *Università di Bari, Bari, Italy*
[c] *Politecnico di Bari, Bari, Italy*

G. Abbiendi [a], A.C. Benvenuti [a], D. Bonacorsi [a,b], S. Braibant-Giacomelli [a,b], L. Brigliadori [a,b], P. Capiluppi [a,b], A. Castro [a,b], F.R. Cavallo [a], M. Cuffiani [a,b], G.M. Dallavalle [a], F. Fabbri [a], A. Fanfani [a,b], D. Fasanella [a,b], P. Giacomelli [a], C. Grandi [a], L. Guiducci [a,b], S. Marcellini [a], G. Masetti [a], M. Meneghelli [a,b,5], A. Montanari [a], F.L. Navarria [a,b], F. Odorici [a], A. Perrotta [a], F. Primavera [a,b], A.M. Rossi [a,b], T. Rovelli [a,b], G.P. Siroli [a,b], R. Travaglini [a,b]

[a] *INFN Sezione di Bologna, Bologna, Italy*
[b] *Università di Bologna, Bologna, Italy*

S. Albergo [a,b], G. Cappello [a,b], M. Chiorboli [a,b], S. Costa [a,b], F. Noto [a], R. Potenza [a,b], M.A. Saizu [a,27], A. Tricomi [a,b], C. Tuve [a,b]

[a] *INFN Sezione di Catania, Catania, Italy*
[b] *Università di Catania, Catania, Italy*

G. Barbagli [a], V. Ciulli [a,b], C. Civinini [a], R. D'Alessandro [a,b], E. Focardi [a,b], S. Frosali [a,b], E. Gallo [a], C. Genta [a], S. Gonzi [a,b], M. Meschini [a], S. Paoletti [a], G. Parrini [a], R. Ranieri [a], G. Sguazzoni [a], A. Tropiano [a,b]

[a] *INFN Sezione di Firenze, Firenze, Italy*
[b] *Università di Firenze, Firenze, Italy*

L. Benussi, S. Bianco, S. Colafranceschi [28], F. Fabbri, D. Piccolo

INFN Laboratori Nazionali di Frascati, Frascati, Italy

P. Fabbricatore, S. Farinon, M. Greco, R. Musenich, S. Tosi

INFN Sezione di Genova, Genova, Italy

A. Benaglia [a,b], L. Carbone [a], P. D'Angelo [a], F. De Guio [a,b], L. Di Matteo [a,b,5], P. Dini [a], F.M. Farina [a,b], S. Fiorendi [a,b], S. Gennai [a,5], A. Ghezzi [a,b], S. Malvezzi [a], R.A. Manzoni [a,b], A. Martelli [a,b], A. Massironi [a,b], D. Menasce [a], L. Moroni [a], P. Negri [a,b,†], M. Paganoni [a,b], D. Pedrini [a], A. Pullia [a,b], S. Ragazzi [a,b], N. Redaelli [a], S. Sala [a], T. Tabarelli de Fatis [a,b]

[a] *INFN Sezione di Milano-Bicocca, Milano, Italy*
[b] *Università di Milano-Bicocca, Milano, Italy*

S. Buontempo [a], C.A. Carrillo Montoya [a], N. Cavallo [a,29], A. De Cosa [a,b,5], O. Dogangun [a,b], F. Fabozzi [a,29], A.O.M. Iorio [a,b], L. Lista [a], S. Meola [a,30], M. Merola [a], P. Paolucci [a,5]

[a] *INFN Sezione di Napoli, Napoli, Italy*
[b] *Università di Napoli "Federico II", Napoli, Italy*

P. Azzi [a], N. Bacchetta [a,5], M. Bellato [a], M. Benettoni [a], M. Biasotto [a,31], D. Bisello [a,b], A. Branca [a,5], R. Carlin [a,b], P. Checchia [a], T. Dorigo [a], U. Dosselli [a], F. Fanzago [a], F. Gasparini [a,b], U. Gasparini [a,b], P. Giubilato [a,b], F. Gonella [a], A. Gozzelino [a], M. Gulmini [a,31], K. Kanishchev [a,c], S. Lacaprara [a], I. Lazzizzera [a,c], M. Loreti [a], M. Margoni [a,b], G. Maron [a,31], M. Mazzucato [a], A.T. Meneguzzo [a,b], F. Montecassiano [a], M. Passaseo [a], J. Pazzini [a,b], M. Pegoraro [a], N. Pozzobon [a,b], P. Ronchese [a,b], F. Simonetto [a,b], E. Torassa [a], M. Tosi [a,b], S. Vanini [a,b], S. Ventura [a], P. Zotto [a,b], G. Zumerle [a,b]

[a] *INFN Sezione di Padova, Padova, Italy*
[b] *Università di Padova, Padova, Italy*
[c] *Università di Trento (Trento), Padova, Italy*

U. Berzano [a], M. Gabusi [a,b], S.P. Ratti [a,b], C. Riccardi [a,b], P. Torre [a,b], P. Vitulo [a,b]

[a] *INFN Sezione di Pavia, Pavia, Italy*
[b] *Università di Pavia, Pavia, Italy*

M. Biasini [a,b], G.M. Bilei [a], L. Fanò [a,b], P. Lariccia [a,b], A. Lucaroni [a,b,5], G. Mantovani [a,b], M. Menichelli [a], A. Nappi [a,b,†], D. Passeri [a,b], P. Placidi [a,b], F. Romeo [a,b], A. Saha [a], A. Santocchia [a,b], L. Servoli [a], A. Spiezia [a,b], S. Taroni [a,b], M. Valdata [a,b]

[a] *INFN Sezione di Perugia, Perugia, Italy*
[b] *Università di Perugia, Perugia, Italy*

F. Angelini [a], S. Arezzini [a], P. Azzurri [a,c], G. Bagliesi [a], A. Basti [a], R. Bellazzini [a], J. Bernardini [a], T. Boccali [a], F. Bosi [a], A. Brez [a], G. Broccolo [a,c], F. Calzolari [a], A. Carboni [a], R. Castaldi [a], C. Cerri [a], A. Ciampa [a], R.T. D'Agnolo [a,c,5], R. Dell'Orso [a], F. Fiori [a,b,5], L. Foà [a,c], A. Giassi [a], S. Giusti [a], A. Kraan [a], L. Latronico [a], F. Ligabue [a,c], S. Linari [a], T. Lomtadze [a], L. Martini [a,32], M. Massa [a], M.M. Massai [a], E. Mazzoni [a], A. Messineo [a,b], A. Moggi [a], F. Palla [a], F. Raffaelli [a], A. Rizzi [a,b], G. Sanguinetti [a], G. Segneri [a], A.T. Serban [a,33], P. Spagnolo [a], G. Spandre [a], P. Squillacioti [a,5], R. Tenchini [a], G. Tonelli [a,b], A. Venturi [a], P.G. Verdini [a]

[a] *INFN Sezione di Pisa, Pisa, Italy*
[b] *Università di Pisa, Pisa, Italy*
[c] *Scuola Normale Superiore di Pisa, Pisa, Italy*

S. Baccaro [a,34], L. Barone [a,b], A. Bartoloni [a], F. Cavallari [a], I. Dafinei [a], D. Del Re [a,b], M. Diemoz [a], C. Fanelli, M. Grassi [a,b,5], E. Longo [a,b], P. Meridiani [a,5], F. Micheli [a,b], S. Nourbakhsh [a,b], G. Organtini [a,b], R. Paramatti [a], S. Rahatlou [a,b], M. Sigamani [a], L. Soffi [a,b], I.G. Talamo [a]

[a] *INFN Sezione di Roma, Roma, Italy*
[b] *Università di Roma "La Sapienza", Roma, Italy*

N. Amapane [a,b], R. Arcidiacono [a,c], S. Argiro [a,b], M. Arneodo [a,c], C. Biino [a], N. Cartiglia [a], M. Costa [a,b], N. Demaria [a], C. Mariotti [a,5], S. Maselli [a], E. Migliore [a,b], V. Monaco [a,b], M. Musich [a,5], M.M. Obertino [a,c], N. Pastrone [a], M. Pelliccioni [a], C. Peroni [a,b], A. Potenza [a,b], A. Romero [a,b], M. Ruspa [a,c], R. Sacchi [a,b], A. Solano [a,b], A. Staiano [a]

[a] *INFN Sezione di Torino, Torino, Italy*
[b] *Università di Torino, Torino, Italy*
[c] *Università del Piemonte Orientale (Novara), Torino, Italy*

F. Ambroglini [a,b], S. Belforte [a], V. Candelise [a,b], M. Casarsa [a], F. Cossutti [a], G. Della Ricca [a,b], B. Gobbo [a], C. Kavka [a], M. Marone [a,b,5], D. Montanino [a,b,5], A. Penzo [a], A. Schizzi [a,b]

[a] *INFN Sezione di Trieste, Trieste, Italy*
[b] *Università di Trieste, Trieste, Italy*

T.Y. Kim, S.K. Nam

Kangwon National University, Chunchon, Republic of Korea

S. Chang, J. Chung, S.W. Ham, D. Han, J. Kang, D.H. Kim, G.N. Kim, J.E. Kim, K.S. Kim, D.J. Kong, M.W. Lee, Y.D. Oh, H. Park, S.R. Ro, D. Son, D.C. Son, J.S. Suh

Kyungpook National University, Daegu, Republic of Korea

J.Y. Kim, Zero J. Kim, S. Song

Chonnam National University, Institute for Universe and Elementary Particles, Kwangju, Republic of Korea

S. Choi, D. Gyun, B. Hong, M. Jo, Y. Jo, M. Kang, H. Kim, T.J. Kim, K.S. Lee, D.H. Moon, S.K. Park, K.S. Sim

Korea University, Seoul, Republic of Korea

M. Choi, G. Hahn, S. Kang, H. Kim, J.H. Kim, C. Park, I.C. Park, S. Park, G. Ryu

University of Seoul, Seoul, Republic of Korea

Y. Choi, Y.K. Choi, J. Goh, M.S. Kim, E. Kwon, B. Lee, J. Lee, S. Lee, H. Seo, I. Yu

Sungkyunkwan University, Suwon, Republic of Korea

M. Janulis, A. Juodagalvis, R. Naujikas

Vilnius University, Vilnius, Lithuania

H. Castilla-Valdez, E. De La Cruz-Burelo, I. Heredia-de La Cruz, R. Lopez-Fernandez, R. Magaña Villalba, J. Martínez-Ortega, A. Sánchez-Hernández, L.M. Villasenor-Cendejas

Centro de Investigacion y de Estudios Avanzados del IPN, Mexico City, Mexico

S. Carrillo Moreno, F. Vazquez Valencia

Universidad Iberoamericana, Mexico City, Mexico

H.A. Salazar Ibarguen

Benemerita Universidad Autonoma de Puebla, Puebla, Mexico

E. Casimiro Linares, A. Morelos Pineda, M.A. Reyes-Santos

Universidad Autónoma de San Luis Potosí, San Luis Potosí, Mexico

P. Allfrey, D. Krofcheck

University of Auckland, Auckland, New Zealand

A.J. Bell, N. Bernardino Rodrigues, A.P.H. Butler, P.H. Butler, R. Doesburg, D. Pfeiffer, S. Reucroft, H. Silverwood, J.C. Williams

University of Canterbury, Christchurch, New Zealand

M. Ahmad, M.H. Ansari, M.I. Asghar, J. Butt, H.R. Hoorani, S. Khalid, W.A. Khan, T. Khurshid, S. Qazi, M.A. Shah, M. Shoaib

National Centre for Physics, Quaid-I-Azam University, Islamabad, Pakistan

H. Bialkowska, B. Boimska, T. Frueboes, R. Gokieli, L. Goscilo, M. Górski, M. Kazana, I.M. Kudla, K. Nawrocki, K. Romanowska-Rybinska, M. Szleper, G. Wrochna, P. Zalewski

National Centre for Nuclear Research, Swierk, Poland

G. Brona, K. Bunkowski, M. Cwiok, H. Czyrkowski, R. Dabrowski, W. Dominik, K. Doroba, A. Kalinowski, M. Konecki, J. Krolikowski, W. Oklinski, K. Pozniak [35], W. Zabolotny [35], P. Zych

Institute of Experimental Physics, Faculty of Physics, University of Warsaw, Warsaw, Poland

G. Kasprowicz, R. Romaniuk

Warsaw University of Technology, Institute of Electronic Systems, Warsaw, Poland

R. Alemany-Fernandez, N. Almeida, P. Bargassa, A. David, P. Faccioli, P.G. Ferreira Parracho, M. Gallinaro, P.Q. Ribeiro, J. Seixas, J. Silva, J. Varela, P. Vischia

Laboratório de Instrumentação e Física Experimental de Partículas, Lisboa, Portugal

S. Afanasiev, I. Belotelov, P. Bunin, Y. Ershov, M. Gavrilenko, A. Golunov, I. Golutvin, N. Gorbounov, I. Gorbunov, I. Gramenitski, V. Kalagin, A. Kamenev, V. Karjavin, V. Konoplyanikov, V. Korenkov, G. Kozlov, A. Kurenkov, A. Lanev, A. Makankin, A. Malakhov, I. Melnitchenko, V.V. Mitsyn, P. Moisenz, D. Oleynik, A. Orlov, V. Palichik, V. Perelygin, A. Petrosyan, M. Savina, R. Semenov, S. Shmatov, S. Shulha, A. Skachkova, N. Skatchkov, V. Smetannikov, V. Smirnov, D. Smolin, E. Tikhonenko, S. Vasil'ev, A. Volodko, A. Zarubin, V. Zhiltsov

Joint Institute for Nuclear Research, Dubna, Russia

S. Evstyukhin, V. Golovtsov, Y. Ivanov, V. Kim, P. Levchenko, V. Murzin, V. Oreshkin, I. Smirnov, V. Sulimov, L. Uvarov, S. Vavilov, A. Vorobyev, An. Vorobyev

Petersburg Nuclear Physics Institute, Gatchina (St. Petersburg), Russia

Yu. Andreev, A. Anisimov, A. Dermenev, S. Gninenko, N. Golubev, D. Gorbunov, A. Karneyeu, M. Kirsanov, N. Krasnikov, V. Matveev, A. Pashenkov, G. Pivovarov, V.E. Postoev, V. Rubakov, V. Shirinyants, A. Solovey, D. Tlisov, A. Toropin, S. Troitsky

Institute for Nuclear Research, Moscow, Russia

V. Epshteyn, M. Erofeeva, V. Gavrilov, V. Kaftanov †, I. Kiselevich, V. Kolosov, A. Konoplyannikov, M. Kossov, Y. Kozlov, A. Krokhotin, D. Litvintsev, N. Lychkovskaya, A. Oulianov, V. Popov, G. Safronov, S. Semenov, N. Stepanov, V. Stolin, E. Vlasov, V. Zaytsev, A. Zhokin

Institute for Theoretical and Experimental Physics, Moscow, Russia

A. Belyaev, E. Boos, V. Bunichev, A. Demiyanov, M. Dubinin [4], L. Dudko, A. Ershov, A. Gribushin, V. Ilyin, A. Kaminskiy [36], V. Klyukhin, O. Kodolova, V. Korotkikh, A. Kryukov, I. Lokhtin, A. Markina, S. Obraztsov, M. Perfilov, S. Petrushanko, A. Popov, A. Proskuryakov, L. Sarycheva †, V. Savrin, A. Snigirev, I. Vardanyan

Moscow State University, Moscow, Russia

V. Andreev, M. Azarkin, I. Dremin, M. Kirakosyan, A. Leonidov, G. Mesyats, S.V. Rusakov, A. Vinogradov

P.N. Lebedev Physical Institute, Moscow, Russia

I. Azhgirey, I. Bayshev, S. Bitioukov, V. Grishin [5], V. Kachanov, A. Kalinin, D. Konstantinov, A. Korablev, V. Krychkine, A. Levine, V. Petrov, A. Ryabov, R. Ryutin, A. Sobol, V. Talov, L. Tourtchanovitch, S. Troshin, N. Tyurin, A. Uzunian, A. Volkov

State Research Center of Russian Federation, Institute for High Energy Physics, Protvino, Russia

P. Adzic [37], M. Djordjevic, M. Ekmedzic, D. Krpic [37], J. Milosevic, N. Smiljkovic, M. Zupan

University of Belgrade, Faculty of Physics and Vinca Institute of Nuclear Sciences, Belgrade, Serbia

M. Aguilar-Benitez, J. Alcaraz Maestre, P. Arce, C. Battilana, E. Calvo, M. Cerrada, M. Chamizo Llatas, N. Colino, B. De La Cruz, A. Delgado Peris, D. Domínguez Vázquez, C. Fernandez Bedoya, J.P. Fernández Ramos, A. Ferrando, J. Flix, M.C. Fouz, P. Garcia-Abia, O. Gonzalez Lopez, S. Goy Lopez, J.M. Hernandez, M.I. Josa, G. Merino, J. Puerta Pelayo, A. Quintario Olmeda, I. Redondo, L. Romero, J. Santaolalla, M.S. Soares, C. Willmott

Centro de Investigaciones Energéticas Medioambientales y Tecnológicas (CIEMAT), Madrid, Spain

C. Albajar, G. Codispoti, J.F. de Trocóniz

Universidad Autónoma de Madrid, Madrid, Spain

H. Brun, J. Cuevas, J. Fernandez Menendez, S. Folgueras, I. Gonzalez Caballero, L. Lloret Iglesias, J. Piedra Gomez

Universidad de Oviedo, Oviedo, Spain

J.A. Brochero Cifuentes, I.J. Cabrillo, A. Calderon, S.H. Chuang, J. Duarte Campderros, M. Felcini [38], M. Fernandez, G. Gomez, J. Gonzalez Sanchez, A. Graziano, C. Jorda, A. Lopez Virto, J. Marco, R. Marco, C. Martinez Rivero, F. Matorras, F.J. Munoz Sanchez, T. Rodrigo, A.Y. Rodríguez-Marrero, A. Ruiz-Jimeno, L. Scodellaro, M. Sobron Sanudo, I. Vila, R. Vilar Cortabitarte

Instituto de Física de Cantabria (IFCA), CSIC-Universidad de Cantabria, Santander, Spain

D. Abbaneo, P. Aspell, E. Auffray, G. Auzinger, M. Bachtis, J. Baechler, P. Baillon, A.H. Ball, D. Barney, J.F. Benitez, C. Bernet [6], W. Bialas, G. Bianchi, P. Bloch, A. Bocci, A. Bonato, C. Botta, H. Breuker, D. Campi, T. Camporesi, E. Cano, G. Cerminara, A. Charkiewicz, T. Christiansen, J.A. Coarasa Perez, B. Curé, D. D'Enterria, A. Dabrowski, J. Daguin, A. De Roeck, S. Di Guida, M. Dobson, N. Dupont-Sagorin, A. Elliott-Peisert, M. Eppard, B. Frisch, W. Funk, A. Gaddi, M. Gastal, G. Georgiou, H. Gerwig, M. Giffels, D. Gigi, K. Gill, D. Giordano, M. Girone, M. Giunta, F. Glege, R. Gomez-Reino Garrido, P. Govoni, S. Gowdy, R. Guida, J. Gutleber, M. Hansen, P. Harris, C. Hartl, J. Harvey, B. Hegner, A. Hinzmann, A. Honma, V. Innocente, P. Janot, K. Kaadze, E. Karavakis, K. Kloukinas, K. Kousouris, P. Lecoq, Y.-J. Lee, P. Lenzi, R. Loos, C. Lourenço, N. Magini, T. Mäki, M. Malberti, L. Malgeri, M. Mannelli, A. Marchioro, J. Marques Pinho Noite, L. Masetti, F. Meijers, S. Mersi, E. Meschi, L. Moneta, M.U. Mozer, M. Mulders, P. Musella, A. Onnela, T. Orimoto, L. Orsini, J.A. Osborne, E. Palencia Cortezon, E. Perez, L. Perrozzi, P. Petagna, A. Petrilli, A. Petrucci, A. Pfeiffer, M. Pierini, M. Pimiä, D. Piparo, G. Polese, H. Postema, L. Quertenmont, A. Racz, W. Reece, D. Ricci, J. Rodrigues Antunes, G. Rolandi [39], C. Rovelli [40], M. Rovere, V. Ryjov, H. Sakulin, D. Samyn, F. Santanastasio, C. Schäfer, C. Schwick, A. Sciaba, I. Segoni, S. Sekmen, A. Sharma, P. Siegrist, P. Silva, M. Simon, P. Sphicas [*,41], D. Spiga, B.G. Taylor, P. Tropea, J. Troska, A. Tsirou, F. Vasey, L. Veillet, G.I. Veres [20], P. Vichoudis, J.R. Vlimant, P. Wertelaers, H.K. Wöhri, S.D. Worm [42], W.D. Zeuner

CERN, European Organization for Nuclear Research, Geneva, Switzerland

W. Bertl, K. Deiters, W. Erdmann, D. Feichtinger, K. Gabathuler, R. Horisberger, Q. Ingram, H.C. Kaestli, S. König, D. Kotlinski, U. Langenegger, B. Meier, F. Meier, D. Renker, T. Rohe, T. Sakhelashvili [43]

Paul Scherrer Institut, Villigen, Switzerland

L. Bäni, F. Behner, B. Betev, B. Blau, P. Bortignon, M.A. Buchmann, B. Casal, N. Chanon, Z. Chen, D.R. Da Silva Di Calafiori, S. Dambach [44], G. Davatz, A. Deisher, G. Dissertori, M. Dittmar, L. Djambazov, M. Donegà, M. Dünser, C. Eggel [44], J. Eugster, G. Faber, K. Freudenreich, C. Grab, W. Hintz, D. Hits, H. Hofer, O. Holme, I. Horvath, P. Lecomte, W. Lustermann, C. Marchica [44], A.C. Marini, P. Martinez Ruiz del Arbol, N. Mohr, F. Moortgat, C. Nägeli [44], P. Nef, F. Nessi-Tedaldi, F. Pandolfi, L. Pape, F. Pauss, M. Peruzzi, T. Punz, F.J. Ronga, U. Röser, M. Rossini, L. Sala, A.K. Sanchez, M.-C. Sawley, D. Schinzel, A. Starodumov [45], B. Stieger, H. Suter, M. Takahashi, L. Tauscher [†], A. Thea, K. Theofilatos, D. Treille, P. Trüb [44], S. Udriot, C. Urscheler, G. Viertel, H.P. von Gunten, R. Wallny, H.A. Weber, L. Wehrli, J. Weng, S. Zelepoukine [46]

Institute for Particle Physics, ETH Zurich, Zurich, Switzerland

C. Amsler [47], V. Chiochia, S. De Visscher, C. Favaro, M. Ivova Rikova, B. Millan Mejias, P. Otiougova, P. Robmann, H. Snoek, S. Tupputi, M. Verzetti

Universität Zürich, Zurich, Switzerland

Y.H. Chang, K.H. Chen, W.T. Chen, A. Go, C.M. Kuo, S.W. Li, W. Lin, M.H. Liu, Z.K. Liu, Y.J. Lu, D. Mekterovic, A.P. Singh, R. Volpe, J.H. Wu, S.S. Yu

National Central University, Chung-Li, Taiwan

P. Bartalini, P. Chang, Y.H. Chang, Y.W. Chang, Y. Chao, K.F. Chen, C. Dietz, Z. Gao [5], U. Grundler, W.-S. Hou, Y. Hsiung, K.Y. Kao, Y.J. Lei, J.j. Liau, S.W. Lin, R.-S. Lu, D. Majumder, E. Petrakou, X. Shi, J.G. Shiu, Y.M. Tzeng, K. Ueno, Y. Velikzhanin, X. Wan, C.C. Wang, M. Wang, J.T. Wei, P. Yeh

National Taiwan University (NTU), Taipei, Taiwan

B. Asavapibhop, N. Srimanobhas

Chulalongkorn University, Bangkok, Thailand

A. Adiguzel, M.N. Bakirci [48], S. Cerci [49], C. Dozen, I. Dumanoglu, E. Eskut, S. Girgis, G. Gokbulut, E. Gurpinar, I. Hos, E.E. Kangal, T. Karaman, G. Karapinar [50], A. Kayis Topaksu, G. Onengut, K. Ozdemir, S. Ozturk [51], A. Polatoz, K. Sogut [52], D. Sunar Cerci [49], B. Tali [49], H. Topakli [48], L.N. Vergili, M. Vergili

Cukurova University, Adana, Turkey

I.V. Akin, T. Aliev, B. Bilin, M. Deniz, H. Gamsizkan, A.M. Guler, K. Ocalan, A. Ozpineci, M. Serin, R. Sever, U.E. Surat, M. Zeyrek

Middle East Technical University, Physics Department, Ankara, Turkey

M. Deliomeroglu, E. Gülmez, B. Isildak [53], M. Kaya [54], O. Kaya [54], S. Ozkorucuklu [55], N. Sonmez [56]

Bogazici University, Istanbul, Turkey

K. Cankocak

Istanbul Technical University, Istanbul, Turkey

B. Grynyov

Institute of Single Crystals of National Academy of Science, Kharkov, Ukraine

L. Levchuk, S. Lukyanenko, D. Soroka, P. Sorokin

National Scientific Center, Kharkov Institute of Physics and Technology, Kharkov, Ukraine

M.K.H. Ahmad, A. Branson, R. McClatchey, M. Odeh, J. Shamdasani, K. Soomro

Centre for Complex Cooperative Systems, University of the West of England, Bristol, United Kingdom

T. Barrass, F. Bostock, J.J. Brooke, E. Clement, D. Cussans, H. Flacher, R. Frazier, J. Goldstein, M. Grimes, G.P. Heath, H.F. Heath, L. Kreczko, W. Lacesso, S. Metson, D.M. Newbold [42], K. Nirunpong, A. Poll, S. Senkin, V.J. Smith, T. Williams

University of Bristol, Bristol, United Kingdom

L. Basso [57], E. Bateman, K.W. Bell, A. Belyaev [57], C. Brew, R.M. Brown, B. Camanzi, D.J.A. Cockerill, J.F. Connolly †, J.A. Coughlan, L.G. Denton, P.S. Flower, M.J. French, R.J.S. Greenhalgh, R.N.J. Halsall, K. Harder, S. Harper, J.A. Hill, J. Jackson, B.W. Kennedy, A.L. Lintern, A.B. Lodge, E. Olaiya, M.R. Pearson, D. Petyt, B.C. Radburn-Smith, C.H. Shepherd-Themistocleous, B.J. Smith, M. Sproston, R. Stephenson, I.R. Tomalin, M.J. Torbet, J.H. Williams †, W.J. Womersley

Rutherford Appleton Laboratory, Didcot, United Kingdom

R. Bainbridge, G. Ball, J. Ballin, D. Bauer, R. Beuselinck, O. Buchmuller, D. Colling, N. Cripps, M. Cutajar, P. Dauncey, G. Davies, M. Della Negra, W. Ferguson, J. Fulcher, D. Futyan, A. Gilbert, A. Guneratne Bryer, G. Hall, Z. Hatherell, J. Hays, G. Iles, M. Jarvis, J. Jones, G. Karapostoli, M. Kenzie, J. Leaver, L. Lyons,

A.-M. Magnan, J. Marrouche, B. Mathias, D.G. Miller, R. Nandi, J. Nash, A. Nikitenko [45], M. Noy, A. Papageorgiou, J. Pela, M. Pesaresi, K. Petridis, M. Pioppi [58], D. Rand, D.M. Raymond, S. Rogerson, A. Rose, M.J. Ryan, C. Seez, P. Sharp †, A. Sparrow, M. Stoye, A. Tapper, C. Timlin, S. Tourneur, M. Vazquez Acosta, T. Virdee, S. Wakefield, N. Wardle, T. Whyntie, M. Wingham, O. Zorba

Imperial College, London, United Kingdom

M. Chadwick, J.E. Cole, P.R. Hobson, A. Khan, P. Kyberd, D. Leggat, D. Leslie, W. Martin, I.D. Reid, P. Symonds, L. Teodorescu, M. Turner

Brunel University, Uxbridge, United Kingdom

J. Dittmann, K. Hatakeyama, H. Liu, T. Scarborough

Baylor University, Waco, USA

O. Charaf, C. Henderson, P. Rumerio

The University of Alabama, Tuscaloosa, USA

A. Avetisyan, T. Bose, E. Carrera Jarrin, C. Fantasia, E. Hazen, A. Heister, J.St. John, P. Lawson, D. Lazic, J. Rohlf, D. Sperka, L. Sulak, F. Varela Rodriguez, S. Wu

Boston University, Boston, USA

J. Alimena, S. Bhattacharya, D. Cutts, Z. Demiragli, A. Ferapontov, A. Garabedian, U. Heintz, R. Hooper, S. Jabeen, G. Kukartsev, E. Laird, G. Landsberg, M. Luk, M. Narain, D. Nguyen, M. Segala, T. Sinthuprasith, T. Speer, K.V. Tsang, Z. Unalan

Brown University, Providence, USA

R. Breedon, G. Breto, M. Calderon De La Barca Sanchez, M. Case, S. Chauhan, M. Chertok, J. Conway, R. Conway, P.T. Cox, J. Dolen, R. Erbacher, M. Gardner, G. Grim, J. Gunion, B. Holbrook, W. Ko, A. Kopecky, R. Lander, F.C. Lin, T. Miceli, P. Murray, M. Nikolic, D. Pellett, F. Ricci-tam, J. Rowe, B. Rutherford, M. Searle, J. Smith, M. Squires, M. Tripathi, R. Vasquez Sierra, R. Yohay

University of California, Davis, Davis, USA

V. Andreev, K. Arisaka, D. Cline, R. Cousins, J. Duris, S. Erhan, P. Everaerts, C. Farrell, J. Hauser, M. Ignatenko, C. Jarvis, J. Kubic, S. Otwinowski, C. Plager, G. Rakness, P. Schlein †, P. Traczyk, V. Valuev, M. Weber, X. Yang, Y. Zheng

University of California, Los Angeles, Los Angeles, USA

J. Babb, R. Clare, M.E. Dinardo, J. Ellison, J.W. Gary, F. Giordano, G. Hanson, G.Y. Jeng [59], J.G. Layter, H. Liu, O.R. Long, A. Luthra, H. Nguyen, S. Paramesvaran, B.C. Shen †, J. Sturdy, S. Sumowidagdo, R. Wilken, S. Wimpenny

University of California, Riverside, Riverside, USA

W. Andrews, J.G. Branson, G.B. Cerati, M. Cinquilli, S. Cittolin, D. Evans, F. Golf, A. Holzner, R. Kelley, M. Lebourgeois, J. Letts, I. Macneill, B. Mangano, T. Martin, A. Mrak-Tadel, S. Padhi, C. Palmer, G. Petrucciani, M. Pieri, M. Sani, I. Sfiligoi, V. Sharma, S. Simon, E. Sudano, M. Tadel, Y. Tu, A. Vartak, S. Wasserbaech [60], F. Würthwein, A. Yagil, J. Yoo

University of California, San Diego, La Jolla, USA

D. Barge, R. Bellan, C. Campagnari, M. D'Alfonso, T. Danielson, K. Flowers, P. Geffert, J. Incandela, C. Justus, P. Kalavase, S.A. Koay, D. Kovalskyi, V. Krutelyov, S. Kyre, S. Lowette, G. Magazzu, N. Mccoll, V. Pavlunin, F. Rebassoo, J. Ribnik, J. Richman, R. Rossin, D. Stuart, W. To, C. West, D. White

University of California, Santa Barbara, Santa Barbara, USA

D. Adamczyk, A. Apresyan, A. Barczyk, A. Bornheim, J. Bunn, Y. Chen, G. Denis, E. Di Marco, J. Duarte, P. Galvez, M. Gataullin, D. Kcira, I. Legrand, V. Litvine, Y. Ma, Z. Maxa, A. Mott, A. Mughal, D. Nae, H.B. Newman, S. Ravot, C. Rogan, S.G. Rozsa, S. Shevchenko, K. Shin, M. Spiropulu, C. Steenberg, M. Thomas, V. Timciuc, F. van Lingen, J. Veverka, B.R. Voicu, R. Wilkinson, S. Xie, Y. Yang, L. Zhang, K. Zhu, R.Y. Zhu

California Institute of Technology, Pasadena, USA

B. Akgun, V. Azzolini, A. Calamba, R. Carroll, T. Ferguson, Y. Iiyama, D.W. Jang, S.Y. Jun, Y.F. Liu, M. Paulini, J. Russ, N. Terentyev, H. Vogel, I. Vorobiev

Carnegie Mellon University, Pittsburgh, USA

J.P. Cumalat, B.R. Drell, W.T. Ford, A. Gaz, B. Heyburn, D. Johnson, E. Luiggi Lopez, U. Nauenberg, J.G. Smith, K. Stenson, K.A. Ulmer, S.R. Wagner, S.L. Zang

University of Colorado at Boulder, Boulder, USA

L. Agostino, J. Alexander, A. Chatterjee, N. Eggert, L.K. Gibbons, B. Heltsley, A. Khukhunaishvili, B. Kreis, V. Kuznetsov, N. Mirman, G. Nicolas Kaufman, J.R. Patterson, D. Riley, A. Ryd, E. Salvati, S. Stroiney, W. Sun, W.D. Teo, J. Thom, J. Thompson, J. Tucker, J. Vaughan, Y. Weng, L. Winstrom, P. Wittich

Cornell University, Ithaca, USA

D. Winn

Fairfield University, Fairfield, USA

S. Abdullin, M. Albert, M. Albrow, J. Anderson, G. Apollinari, M. Atac [†], W. Badgett, J.A. Bakken, B. Baldin, K. Banicz, L.A.T. Bauerdick, A. Beretvas, J. Berryhill, P.C. Bhat, M. Binkley [†], F. Borcherding, K. Burkett, J.N. Butler, V. Chetluru, H.W.K. Cheung, F. Chlebana, S. Cihangir, W. Dagenhart, G. Derylo, C. Dumitrescu, D. Dykstra, D.P. Eartly, J.E. Elias [†], V.D. Elvira, G. Eulisse, D. Evans, D. Fagan, I. Fisk, S. Foulkes, J. Freeman, I. Gaines, Y. Gao, P. Gartung, L. Giacchetti, E. Gottschalk, D. Green, Y. Guo, O. Gutsche, A. Hahn, J. Hanlon, R.M. Harris, J. Hirschauer, B. Holzman, B. Hooberman, J. Howell, C.h. Huang, D. Hufnagel, S. Jindariani, M. Johnson, C.D. Jones, U. Joshi, E. Juska, B. Kilminster, B. Klima, S. Kunori, S. Kwan, K. Larson, C. Leonidopoulos, J. Linacre, D. Lincoln, R. Lipton, J.A. Lopez Perez, S. Los, J. Lykken, K. Maeshima, J.M. Marraffino, S. Maruyama, D. Mason, P. McBride, T. McCauley, K. Mishra, S. Moccia, R.K. Mommsen, S. Mrenna, Y. Musienko [61], S. Muzaffar, C. Newman-Holmes, V. O'Dell, I. Osborne, J. Pivarski, S. Popescu [27], R. Pordes, O. Prokofyev, V. Rapsevicius, A. Ronzhin, P. Rossman, S. Ryu, E. Sexton-Kennedy, S. Sharma, T.M. Shaw, R.P. Smith [†], A. Soha, W.J. Spalding, L. Spiegel, W. Tanenbaum, L. Taylor, R. Thompson, A. Tiradani, S. Tkaczyk, N.V. Tran, L. Tuura, L. Uplegger, E.W. Vaandering, R. Vidal, J. Whitmore, W. Wu, F. Yang, J. Yarba, J.C. Yun, T. Zimmerman

Fermi National Accelerator Laboratory, Batavia, USA

D. Acosta, P. Avery, V. Barashko, D. Bourilkov, M. Chen, T. Cheng, S. Das, M. De Gruttola, G.P. Di Giovanni, D. Dobur, S. Dolinsky, A. Drozdetskiy, R.D. Field, M. Fisher, Y. Fu, I.K. Furic, J. Gartner, L. Gorn, D. Holmes, J. Hugon, B. Kim, J. Konigsberg, A. Korytov, A. Kropivnitskaya, T. Kypreos, J.F. Low, A. Madorsky, K. Matchev, P. Milenovic [62], G. Mitselmakher, L. Muniz, M. Park, R. Remington, A. Rinkevicius, B. Scurlock, N. Skhirtladze, M. Snowball, J. Stasko, J. Yelton, M. Zakaria

University of Florida, Gainesville, USA

V. Gaultney, S. Hewamanage, L.M. Lebolo, S. Linn, P. Markowitz, G. Martinez, J.L. Rodriguez

Florida International University, Miami, USA

T. Adams, A. Askew, M. Bertoldi, J. Bochenek, J. Chen, W.G.D. Dharmaratna, B. Diamond, S.V. Gleyzer, J. Haas, S. Hagopian, V. Hagopian, M. Jenkins, K.F. Johnson, H. Prosper, S. Tentindo, V. Veeraraghavan, M. Weinberg

Florida State University, Tallahassee, USA

M.M. Baarmand, B. Dorney, M. Hohlmann, H. Kalakhety, R. Ralich, I. Vodopiyanov, F. Yumiceva

Florida Institute of Technology, Melbourne, USA

M.R. Adams, I.M. Anghel, L. Apanasevich, Y. Bai, V.E. Bazterra, R.R. Betts, I. Bucinskaite, J. Callner, R. Cavanaugh, M.H. Chung, O. Evdokimov, E.J. Garcia-Solis, L. Gauthier, C.E. Gerber, D.J. Hofman, R. Hollis, A. Iordanova, S. Khalatyan, G.J. Kunde [63], F. Lacroix, M. Malek, C. O'Brien, C. Silkworth, C. Silvestre, A. Smoron, D. Strom, P. Turner, N. Varelas

University of Illinois at Chicago (UIC), Chicago, USA

U. Akgun, E.A. Albayrak, A.S. Ayan, B. Bilki [64], W. Clarida, P. Debbins, F. Duru, F.D. Ingram, E. McCliment, J.-P. Merlo, H. Mermerkaya [65], A. Mestvirishvili, M.J. Miller, A. Moeller, J. Nachtman, C.R. Newsom, E. Norbeck, J. Olson, Y. Onel, F. Ozok [66], I. Schmidt, S. Sen, P. Tan, E. Tiras, J. Wetzel, T. Yetkin, K. Yi

The University of Iowa, Iowa City, USA

B.A. Barnett, B. Blumenfeld, S. Bolognesi, D. Fehling, G. Giurgiu, A.V. Gritsan, Z.J. Guo, G. Hu, P. Maksimovic, S. Rappoccio, M. Swartz, A. Whitbeck

Johns Hopkins University, Baltimore, USA

P. Baringer, A. Bean, G. Benelli, D. Coppage, O. Grachov, R.P. Kenny Iii, M. Murray, D. Noonan, V. Radicci, S. Sanders, R. Stringer, G. Tinti, J.S. Wood, V. Zhukova

The University of Kansas, Lawrence, USA

A.F. Barfuss, T. Bolton, I. Chakaberia, A. Ivanov, S. Khalil, M. Makouski, Y. Maravin, S. Shrestha, I. Svintradze

Kansas State University, Manhattan, USA

J. Gronberg, D. Lange, D. Wright

Lawrence Livermore National Laboratory, Livermore, USA

A. Baden, R. Bard, M. Boutemeur, B. Calvert, S.C. Eno, J.A. Gomez, T. Grassi, N.J. Hadley, R.G. Kellogg, M. Kirn, T. Kolberg, Y. Lu, M. Marionneau, A.C. Mignerey, K. Pedro, A. Peterman, K. Rossato, A. Skuja, J. Temple, M.B. Tonjes, S.C. Tonwar, T. Toole, E. Twedt

University of Maryland, College Park, USA

A. Apyan, G. Bauer, J. Bendavid, W. Busza, E. Butz, I.A. Cali, M. Chan, V. Dutta, G. Gomez Ceballos, M. Goncharov, K.A. Hahn, Y. Kim, M. Klute, K. Krajczar [67], A. Levin, P.D. Luckey, T. Ma, S. Nahn, C. Paus, D. Ralph, C. Roland, G. Roland, M. Rudolph, G.S.F. Stephans, F. Stöckli, K. Sumorok, K. Sung, D. Velicanu, E.A. Wenger, R. Wolf, B. Wyslouch, M. Yang, Y. Yilmaz, A.S. Yoon, M. Zanetti

Massachusetts Institute of Technology, Cambridge, USA

D. Bailleux, S.I. Cooper, P. Cushman, B. Dahmes, A. De Benedetti, R. Egeland, G. Franzoni, A. Gude, J. Haupt, A. Inyakin, S.C. Kao, K. Klapoetke, Y. Kubota, J. Mans, N. Pastika, R. Rusack, A. Singovsky, N. Tambe, J. Turkewitz

University of Minnesota, Minneapolis, USA

L.M. Cremaldi, R. Kroeger, L. Perera, R. Rahmat, J. Reidy, D.A. Sanders, D. Summers

University of Mississippi, University, USA

G. Attebury, E. Avdeeva, K. Bloom, B. Bockelman, S. Bose, D.R. Claes, A. Dominguez, M. Eads, J. Keller, I. Kravchenko, J. Lazo-Flores, C. Lundstedt, H. Malbouisson, S. Malik, R. Snihur, G.R. Snow, D. Swanson

University of Nebraska-Lincoln, Lincoln, USA

U. Baur, A. Godshalk, I. Iashvili, S. Jain, A. Kharchilava, A. Kumar, S.P. Shipkowski, K. Smith

State University of New York at Buffalo, Buffalo, USA

G. Alverson, E. Barberis, D. Baumgartel, M. Chasco, J. Haley, J. Moromisato, D. Nash, J. Swain, D. Trocino, E. Von Goeler, D. Wood, J. Zhang

Northeastern University, Boston, USA

A. Anastassov, B. Gobbi, A. Kubik, L. Lusito, N. Odell, R.A. Ofierzynski, B. Pollack, A. Pozdnyakov, M. Schmitt, S. Stoynev, M. Velasco, S. Won

Northwestern University, Evanston, USA

L. Antonelli, B. Baumbaugh, D. Berry, A. Brinkerhoff, K.M. Chan, A.H. Heering, M. Hildreth, C. Jessop, D.J. Karmgard, N. Kellams, J. Kolb, K. Lannon, W. Luo, S. Lynch, N. Marinelli, D.M. Morse, T. Pearson, M. Planer, R. Ruchti, J. Slaunwhite, N. Valls, M. Wayne, M. Wolf, A. Woodard

University of Notre Dame, Notre Dame, USA

B. Bylsma, L.S. Durkin, C. Hill, R. Hughes, K. Kotov, T.Y. Ling, D. Puigh, M. Rodenburg, C.J. Rush, V. Sehgal, C. Vuosalo, G. Williams, B.L. Winer

The Ohio State University, Columbus, USA

N. Adam, E. Berry, P. Elmer, D. Gerbaudo, V. Halyo, P. Hebda, J. Hegeman, A. Hunt, P. Jindal, D. Lopes Pegna, P. Lujan, D. Marlow, T. Medvedeva, M. Mooney, J. Olsen, P. Piroué, X. Quan, A. Raval, H. Saka, D. Stickland, C. Tully, J.S. Werner, T. Wildish, Z. Xie, S.C. Zenz, A. Zuranski

Princeton University, Princeton, USA

J.G. Acosta, M. Bonnett Del Alamo, E. Brownson, X.T. Huang, A. Lopez, H. Mendez, S. Oliveros, J.E. Ramirez Vargas, A. Zatserklyaniy

University of Puerto Rico, Mayaguez, USA

E. Alagoz, K. Arndt, V.E. Barnes, D. Benedetti, G. Bolla, D. Bortoletto, A. Bujak, M. De Mattia, A. Everett, L. Gutay, Z. Hu, M. Jones, O. Koybasi, M. Kress, A.T. Laasanen, J. Lee, N. Leonardo, C. Liu, V. Maroussov, P. Merkel, D.H. Miller, J. Miyamoto, N. Neumeister, C. Rott, A. Roy, I. Shipsey, D. Silvers, A. Svyatkovskiy, M. Vidal Marono, H.D. Yoo, J. Zablocki, Y. Zheng

Purdue University, West Lafayette, USA

S. Guragain, N. Parashar

Purdue University Calumet, Hammond, USA

A. Adair, C. Boulahouache, V. Cuplov, K.M. Ecklund, F.J.M. Geurts, S.J. Lee, W. Li, J.H. Liu, M. Matveev, B.P. Padley, R. Redjimi, J. Roberts, A. Tumanov, P. Yepes, J. Zabel

Rice University, Houston, USA

B. Betchart, A. Bodek, H. Budd, Y.S. Chung, R. Covarelli, P. de Barbaro, R. Demina, Y. Eshaq, T. Ferbel, A. Garcia-Bellido, G. Ginther, P. Goldenzweig, Y. Gotra, J. Han, A. Harel, S. Korjenevski, D.C. Miner, D. Orbaker, W. Sakumoto, P. Slattery, D. Vishnevskiy, M. Zielinski

University of Rochester, Rochester, USA

A. Bhatti, R. Ciesielski, L. Demortier, K. Goulianos, G. Lungu, S. Malik, C. Mesropian

The Rockefeller University, New York, USA

S. Arora, A. Barker, J.P. Chou, C. Contreras-Campana, E. Contreras-Campana, D. Duggan, D. Ferencek, Y. Gershtein, R. Gray, E. Halkiadakis, D. Hidas, A. Lath, S. Panwalkar, M. Park, R. Patel, V. Rekovic, J. Robles, K. Rose, S. Salur, S. Schnetzer, C. Seitz, S. Somalwar, R. Stone, S. Thomas

Rutgers, the State University of New Jersey, Piscataway, USA

G. Cerizza, M. Hollingsworth, G. Ragghianti, S. Spanier, Z.C. Yang, A. York

University of Tennessee, Knoxville, USA

O. Bouhali, R. Eusebi, W. Flanagan, J. Gilmore, T. Kamon [68], V. Khotilovich, R. Montalvo, C.N. Nguyen, I. Osipenkov, Y. Pakhotin, A. Perloff, J. Roe, A. Safonov, T. Sakuma, S. Sengupta, I. Suarez, A. Tatarinov, D. Toback

Texas A&M University, College Station, USA

N. Akchurin, J. Damgov, C. Dragoiu, P.R. Dudero, C. Jeong, K. Kovitanggoon, S.W. Lee, T. Libeiro, Y. Roh, A. Sill, I. Volobouev, R. Wigmans

Texas Tech University, Lubbock, USA

E. Appelt, A.G. Delannoy, D. Engh, C. Florez, W. Gabella, S. Greene, A. Gurrola, W. Johns, P. Kurt, C. Maguire, A. Melo, M. Sharma, P. Sheldon, B. Snook, S. Tuo, J. Velkovska

Vanderbilt University, Nashville, USA

D. Andelin, M.W. Arenton, M. Balazs, S. Boutle, S. Conetti, B. Cox, B. Francis, J. Goodell, R. Hirosky, A. Ledovskoy, C. Lin, C. Neu, D. Phillips II, J. Wood

University of Virginia, Charlottesville, USA

S. Gollapinni, R. Harr, P.E. Karchin, C. Kottachchi Kankanamge Don, P. Lamichhane, M. Mattson, C. Milstène, A. Sakharov

Wayne State University, Detroit, USA

M. Anderson, D. Belknap, J.N. Bellinger, L. Borrello, D. Bradley, D. Carlsmith, M. Cepeda, I. Crotty [5], S. Dasu, F. Feyzi, E. Friis, T. Gorski, L. Gray, K.S. Grogg, M. Grothe, R. Hall-Wilton, M. Herndon, A. Hervé, P. Klabbers, J. Klukas, J. Lackey, A. Lanaro, C. Lazaridis, J. Leonard, R. Loveless, S. Lusin [5], M. Magrans de Abril, W. Maier, A. Mohapatra, I. Ojalvo, F. Palmonari, G.A. Pierro, D. Reeder, I. Ross, A. Savin, W.H. Smith, J. Swanson, D. Wenman

University of Wisconsin, Madison, USA

* Corresponding author.
† Deceased.
[1] Also at Vienna University of Technology, Vienna, Austria.
[2] Also at National Institute of Chemical Physics and Biophysics, Tallinn, Estonia.
[3] Also at Universidade Federal do ABC, Santo Andre, Brazil.
[4] Also at California Institute of Technology, Pasadena, USA.
[5] Also at CERN, European Organization for Nuclear Research, Geneva, Switzerland.
[6] Also at Laboratoire Leprince-Ringuet, Ecole Polytechnique, IN2P3–CNRS, Palaiseau, France.
[7] Also at Suez Canal University, Suez, Egypt.
[8] Also at Zewail City of Science and Technology, Zewail, Egypt.

[9] Also at Cairo University, Cairo, Egypt.
[10] Also at Fayoum University, El-Fayoum, Egypt.
[11] Also at British University, Cairo, Egypt.
[12] Now at Ain Shams University, Cairo, Egypt.
[13] Also at National Centre for Nuclear Research, Swierk, Poland.
[14] Also at Université de Haute-Alsace, Mulhouse, France.
[15] Also at Joint Institute for Nuclear Research, Dubna, Russia.
[16] Also at Moscow State University, Moscow, Russia.
[17] Also at Brandenburg University of Technology, Cottbus, Germany.
[18] Also at The University of Kansas, Lawrence, USA.
[19] Also at Institute of Nuclear Research ATOMKI, Debrecen, Hungary.
[20] Also at Eötvös Loránd University, Budapest, Hungary.
[21] Also at Tata Institute of Fundamental Research – HECR, Mumbai, India.
[22] Now at King Abdulaziz University, Jeddah, Saudi Arabia.
[23] Also at University of Visva-Bharati, Santiniketan, India.
[24] Also at Sharif University of Technology, Tehran, Iran.
[25] Also at Isfahan University of Technology, Isfahan, Iran.
[26] Also at Plasma Physics Research Center, Science and Research Branch, Islamic Azad University, Teheran, Iran.
[27] Also at Horia Hulubei National Institute of Physics and Nuclear Engineering (IFIN-HH), Bucharest, Romania.
[28] Also at Facoltà Ingegneria Università di Roma, Roma, Italy.
[29] Also at Università della Basilicata, Potenza, Italy.
[30] Also at Università degli Studi Guglielmo Marconi, Roma, Italy.
[31] Also at Laboratori Nazionali di Legnaro dell' INFN, Legnaro, Italy.
[32] Also at Università degli Studi di Siena, Siena, Italy.
[33] Also at University of Bucharest, Faculty of Physics, Bucuresti-Magurele, Romania.
[34] Also at ENEA – Casaccia Research Center, S. Maria di Galeria, Italy.
[35] Also at Warsaw University of Technology, Institute of Electronic Systems, Warsaw, Poland.
[36] Also at INFN Sezione di Padova; Università di Padova; Università di Trento (Trento), Padova, Italy.
[37] Also at Faculty of Physics of University of Belgrade, Belgrade, Serbia.
[38] Also at University of California, Los Angeles, Los Angeles, USA.
[39] Also at Scuola Normale e Sezione dell'INFN, Pisa, Italy.
[40] Also at INFN Sezione di Roma; Università di Roma "La Sapienza", Roma, Italy.
[41] Also at University of Athens, Athens, Greece.
[42] Also at Rutherford Appleton Laboratory, Didcot, United Kingdom.
[43] Also at Institute of High Energy Physics and Informatization, Tbilisi State University, Tbilisi, Georgia.
[44] Also at Paul Scherrer Institut, Villigen, Switzerland.
[45] Also at Institute for Theoretical and Experimental Physics, Moscow, Russia.
[46] Also at University of Wisconsin, Madison, USA.
[47] Also at Albert Einstein Center for Fundamental Physics, Bern, Switzerland, BERN, SWITZERLAND.
[48] Also at Gaziosmanpasa University, Tokat, Turkey.
[49] Also at Adiyaman University, Adiyaman, Turkey.
[50] Also at Izmir Institute of Technology, Izmir, Turkey.
[51] Also at The University of Iowa, Iowa City, USA.
[52] Also at Mersin University, Mersin, Turkey.
[53] Also at Ozyegin University, Istanbul, Turkey.
[54] Also at Kafkas University, Kars, Turkey.
[55] Also at Suleyman Demirel University, Isparta, Turkey.
[56] Also at Ege University, Izmir, Turkey.
[57] Also at School of Physics and Astronomy, University of Southampton, Southampton, United Kingdom.
[58] Also at INFN Sezione di Perugia; Università di Perugia, Perugia, Italy.
[59] Also at University of Sydney, Sydney, Australia.
[60] Also at Utah Valley University, Orem, USA.
[61] Also at Institute for Nuclear Research, Moscow, Russia.
[62] Also at University of Belgrade, Faculty of Physics and Vinca Institute of Nuclear Sciences, Belgrade, Serbia.
[63] Also at Los Alamos National Laboratory, Los Alamos, USA.
[64] Also at Argonne National Laboratory, Argonne, USA.
[65] Also at Erzincan University, Erzincan, Turkey.
[66] Also at Mimar Sinan University, Istanbul, Istanbul, Turkey.
[67] Also at KFKI Research Institute for Particle and Nuclear Physics, Budapest, Hungary.
[68] Also at Kyungpook National University, Daegu, Republic of Korea.